

1 Late Quaternary spatial and temporal variability in Arctic deep-
2 sea bioturbation and its relation to Mn cycles

3

4

5 Löwemark, L.^{1,2*}, O'Regan, M.^{1,3}, Hanebuth, T.J.J.⁴, Jakobsson, M.¹

6

7 ¹*Department of Geological Sciences, Stockholm University, 106 91 Stockholm,*

8 *Sweden*

9 ²*Alfred Wegener Institute for Polar and Marine Research, Climate Science Division,*

10 *27570 Bremerhaven, Germany, Tel.: +49 (0)471-4831-1881, Fax: +49 (0)471-4831-*

11 *1797*

12 ³*School of Earth & Ocean Sciences, Cardiff University, UK, 44 (0) 29 208 766209,*

13 *Fax: +44 (0) 29 208 74326*

14 ⁴*MARUM – Center for Marine Environmental Sciences, University of Bremen,*

15 *Germany, Tel.: +49-(0)421 218 – 65200, Fax: +49-(0)421 218 - 65515*

16

17 *Corresponding author

18

19

20 **ABSTRACT**

21 Changes in intensity and composition of bioturbation and trace fossils in deep-

22 sea settings are directly related to changes in environmental parameters such as food

23 availability, bottom water oxygenation, or substrate consistency. Because trace fossils

24 are practically always preserved *in situ*, and are often present in environments where
25 other environmental indicators are scarce or may have been compromised or removed
26 by diagenetic processes, the trace fossils provide an important source of
27 paleoenvironmental information in regions such as the deep Arctic Ocean. Detailed
28 analysis of X-ray radiographs from 12 piston and gravity cores from a transect
29 spanning from the Makarov Basin to the Yermak Plateau via the Lomonosov Ridge,
30 the Morris Jesup Rise, and the Gakkel Ridge reveal both spatial and temporal
31 variations in an ichnofauna consisting of *Chondrites*, *Nereites*, *Phycosiphon*,
32 *Planolites*, *Scolicia*, *Trichichnus*, *Zoophycos*, as well as deformational biogenic
33 structures. The spatial variability in abundance and diversity are in close
34 correspondence to observed patterns in the distribution of modern benthos, suggesting
35 that food availability and food flux to the sea floor are the most important parameters
36 controlling variations in bioturbation in the Arctic Ocean. The most diverse
37 ichnofaunas were observed at sites on the central Lomonosov Ridge that today have
38 partially ice free conditions and relatively high summer productivity. In contrast, the
39 most sparse ichnofauna was observed in the ice-infested region on the Lomonosov
40 Ridge north of Greenland. Since primary productivity, and therefore also the food flux
41 at a certain location, is ultimately controlled by the geographical position in relation to
42 ice margin and the continental shelves, temporal variations in abundance and diversity
43 of trace fossils have the potential to reveal changes in food flux, and consequently sea
44 ice conditions on glacial-interglacial time scales. Down core analysis reveal clearly
45 increased abundance and diversity during interglacial/interstadial intervals that were
46 identified through strongly enhanced Mn levels and the presence of micro- and
47 nanofossils. Warm stages are characterized by larger trace fossils such as *Scolicia*,
48 *Planolites* or *Nereites*, while cold stages typically display an ichnofauna dominated by

49 small deep penetrating trace fossils such as *Chondrites* or *Trichichnus*. The presence
50 of biogenic structures in glacial intervals clearly show that the Arctic deep waters
51 must have remained fairly well ventilated also during glacials, thereby lending
52 support to the hypothesis that the conspicuous brown layers rich in Mn which are
53 found ubiquitously over the Arctic basins are related to input from rivers and coastal
54 erosion during sea level high-stands rather than redox processes in the water column
55 and on the sea floor. However, the X-ray radiograph study also revealed the presence
56 of apparently post-sedimentary, diagenetically formed Mn-layers which are not
57 directly related to Mn input from rivers and shelves. These observations thus bolster
58 the hypothesis that the bioturbated, brownish Mn-rich layers can be used for
59 stratigraphic correlation over large distances in the Arctic Ocean, but only if post
60 sedimentary diagenetic layers can be identified and accounted for in the Mn-cycle
61 stratigraphy.

62

63 Keywords: bioturbation, trace fossils, Arctic Ocean, diagenesis, Manganese

64 **1 Introduction**

65 Variations in the type and intensity of bioturbation in Arctic sediments have
66 been studied from sea-floor photographs (e.g., Kitchell, 1979; Kitchell et al., 1978;
67 MacDonald et al., 2010), and down-core variations in trace fossils and lebensspuren
68 have been noted in several previous studies, (e.g., Clark et al., 1980; Phillips and
69 Grantz, 1997; Scott et al., 1989). However, despite the relatively large number of
70 cores now available from the deep Arctic Ocean (Stein, 2008), no systematic studies
71 on Arctic deep-sea ichnology have been published. Here we present the first detailed
72 ichnological studies of spatial and temporal variation in the composition of the Arctic

73 Ocean ichnofauna, and focus on how observed changes may be related to past
74 changes in circulation and sea-ice coverage.

75 Because the composition and activities of the benthic fauna is determined by
76 parameters such as food flux or availability, bottom water oxygenation, and substrate
77 consistency, downcore variations in the traces left by the organisms can be used as
78 proxies to reconstruct past variations in environmental conditions (e.g., Savrda, 2007;
79 Wetzel, 1991). Trace fossils have certain advantages over other environmental proxies
80 as they are preserved *in situ* and cannot be redistributed and therefore by necessity
81 reflect the environment at the position where they are found. Furthermore, trace
82 fossils are commonly preserved in settings where other proxies are missing or have
83 been obliterated, in fact, they are quite resistant to diagenetic processes which often
84 act to even enhance their visibility. However, in unlithified, homogeneously coloured
85 sediment, trace fossils can sometimes be hard to make out. Here X-ray radiographs of
86 the sediment offer a powerful tool to reveal both physical and biological structures in
87 the sediment that would otherwise be invisible to the naked eye (cf. Bouma, 1964).
88 These characteristics make trace fossils particularly promising in regions such as the
89 Arctic Ocean where dating and paleoceanographic reconstructions are difficult due to
90 the scarcity of nanno- and microfossils, a complex magnetostratigraphy (Backman et
91 al., 2009; Spielhagen et al., 2004), and problematic absolute dating methods (e.g., ^{14}C
92 and ^{10}Be , Sellén et al., 2009)

93 In an effort to address the dating problem, it has been argued that the recurrent
94 downhole occurrence of strongly bioturbated, brownish (enriched in Mn) intervals in
95 many central Arctic Ocean sediments provides a possibility for age control, as these
96 cycles could be correlated to the low-latitude stable oxygen isotope curve (Jakobsson
97 et al., 2000). Following IODP Expedition 302 to the Lomonosov Ridge (the Arctic

98 Coring Expedition – ACEX), downhole variations in Mn content in Quaternary
99 sediments were shown to be strongly correlated to cyclostratigraphic changes in the
100 physical, chemical and magnetic properties of the sediments, and were found to
101 coincide with occurrences of agglutinated benthic forams, supporting the assertion
102 that Mn enrichment occurs during interglacial/interstadial periods throughout the
103 middle and latter part of the Quaternary (O'Regan et al., 2008; O'Regan et al., 2010).

104 Three main mechanisms have been proposed to explain the observed cyclicity
105 in Mn enrichment: 1) variations in deep-water circulation causing precipitation or
106 dissolution of Mn; 2) variations in the input of Mn to the Arctic Ocean; and 3)
107 diagenetic processes redistributing the Mn within the sediment (e.g., Jakobsson et al.,
108 2000; Löwemark et al., 2008; Macdonald and Gobeil, 2011; März et al., 2011). Here
109 detailed studies of variations in deep sea bioturbation in combination with sediment
110 geochemical analysis may provide information on the relative importance of the
111 different processes, a prerequisite for an improved understanding of the Arctic
112 paleoclimate system.

113 The aims of this study therefore are to: a) perform the first inventory of deep
114 marine Arctic trace fossils and their spatial and temporal variability, b) study the
115 genetic relationship between bioturbation and the Mn-rich layers, and c) elucidate the
116 environmental implications from the observed patterns in trace fossil distribution.

117 **2 Background**

118 *2.1 Arctic hydrography*

119 The Arctic Ocean is a semi-confined ocean with over half its area composed of
120 shallow shelves (Fig. 1) (Jakobsson et al., 2003), and a narrow opening at the Fram
121 Strait which provides the only deep-water connection to the World Ocean. These
122 features make the Arctic Ocean especially sensitive to glaciations and associated sea-

123 level changes. The Arctic Ocean is separated into the Amerasian Basin and the
124 Eurasian Basin by the Lomonosov Ridge. The Lomonosov Ridge is a sliver of
125 continental crust rifted from the Eurasian continent about 55 Ma (Jokat et al., 1992)
126 and rises steeply from the abyssal plains with depths of 3-5 km up to about 1000 m
127 below the sea surface. It therefore acts like a barrier between the two basins resulting
128 in considerably longer residence times for the deep waters in the Amerasian Basin
129 (Tomczak and Godfrey, 2002). In the central part of the ridge, a bathymetric
130 depression forms an intra-ridge basin, the so-called intrabasin. This intrabasin is
131 connected to the Makarov Basin on the Amerasian side and the Amundsen Basin on
132 the Eurasian side through relatively narrow channels with sill depths of about 1800 m
133 (Björk et al., 2010; Björk et al., 2007). These conduit allows an exchange between the
134 otherwise isolated deep waters of the two basins. The Lomonosov Ridge also forces
135 the intermediate waters of Atlantic origin to form a cyclonic gyre in the Eurasian
136 basin. On its way through the Eurasian basin the Arctic intermediate water is mixed
137 with extremely cold waters that form on the shelves during sea ice formation. This
138 cold and dense water then leaves the Arctic Ocean through the Fram Strait to form an
139 important part of the global thermohaline circulation (Meincke et al., 1997; Tomczak
140 and Godfrey, 2002). Surface and halocline water properties in the Eurasian Basin are
141 mainly controlled by the inflow of Atlantic waters through the Fram Strait and via the
142 Barents Sea, and mixing processes on the shelf areas (Rudels et al., 2004).

143 The surface circulation of the Arctic Ocean is dominated by the wind driven
144 Beaufort Gyre over the Amerasian Basin and the Transpolar Drift that transports sea
145 ice across the Eurasian Basin from the Siberian shelves to the Fram Strait. Sea ice is
146 the main transporting agent for particles larger than clay and the position of the
147 boundary between the Beaufort Gyre and the Transpolar Drift consequently has an

148 important role in controlling the composition of sediments deposited in the central
149 Arctic region (e.g. Sellén et al., 2010). Today, primary productivity in the central
150 Arctic Ocean is dominated by phytoplankton and ice-algae (Horner and Schrader,
151 1982) and almost all primary productivity takes place during the spring/summer
152 season in open leads or under the thinner first year ice (Arrigo et al., 2012; Arrigo et
153 al., 2008).

154 *2.2 Arctic macrobenthos*

155 Although the Arctic basin is considerably understudied in comparison to other
156 oceans, several larger studies were performed in recent years addressing variation and
157 abundance of benthic fauna from the shelves to the deep basins (e.g. Clough et al.,
158 1997; Kröncke, 1994; MacDonald et al., 2010; Vanreusel et al., 2000). The results
159 suggest that the fauna of the deep-sea floor is more diverse than previously believed.
160 Biomass and macrofaunal diversity was found to be comparable to the lower end of
161 the spectrum observed in other oligotrophic regions of the world (Piepenburg, 2005;
162 Vanreusel et al., 2000). Although the organisms vary from site to site, significant
163 regional differences exist (Renaud et al., 2006). Most studies found that the benthic
164 fauna was dominated by polychaetes, crustaceans, echinodermata and bivalves
165 (Bluhm et al., 2005; Deubel, 2000; MacDonald et al., 2010). Polychaetes being the
166 most common in terms of abundance and taxon number (MacDonald et al., 2010).
167 This dominance of polychaetes was especially apparent at deeper stations. Sea-floor
168 photographs along a transect from the Chukchi Borderland to the Amerasian abyssal
169 plain showed lebensspuren such as solitary holes, gastropod and crustacean tracks, as
170 well as different trails at all stations (MacDonald et al., 2010).

171 The macrofauna in the Arctic Ocean is mostly of Atlantic type, and only a few
172 endemic species are found (Kröncke, 1994). However, true species diversity is still

173 poorly known due to the sparse sampling density - the first quantitative megafauna
174 studies were published in 2010 (MacDonald et al., 2010). Most of the benthic
175 organisms found were deposit feeders, but increased numbers of suspension feeders
176 were reported from rises such as the flanks of the Lomonosov Ridge (Deubel, 2000;
177 Iken et al., 2005; Kröncke, 1998; Piepenburg, 2005). Food web structure studies based
178 on $\delta^{13}\text{C}$ and $\delta^{15}\text{N}$ also showed that many benthic organisms were deposit feeders and
179 that they use refractory organic material to a large extent in their metabolism (Iken et
180 al., 2005).

181 These studies show a general pattern where biomass, abundance and diversity
182 of the benthic fauna is inversely correlated with water depth and latitude, where
183 latitude is a measure of the distance to the shelves and ice-margin (Bluhm et al., 2005;
184 Clough et al., 1997; MacDonald et al., 2010; Piepenburg, 2005; Renaud et al., 2006;
185 Van Averbek et al., 1997). Similar results have been obtained from studies of benthic
186 foraminifer (Wollenburg and Kuhnt, 2000) and ostracode (Cronin et al., 2010)
187 distributions. Some studies noted an increase in biomass and abundances towards the
188 Lomonosov Ridge (Clough et al., 1997; Kröncke, 1994), possibly related to a lateral
189 input of organic material by ocean circulation along the slope of the ridge.

190 *2.3 Arctic sediments*

191 Arctic Ocean sediments differ from the general oceanic sediments in several
192 ways. The sediments show extreme variations in grain size, varying from hemipelagic
193 muds to coarse-grained ice rafted debris (IRD), with maximum IRD content
194 characteristically occurring in intervals corresponding to late glacial and deglacial
195 intervals (Phillips and Grantz, 2001). There are also larger spatial and temporal
196 variations in sedimentation rates than typically found in the open oceans because of
197 variations in the transport paths of sea ice and icebergs. The processes delivering

198 sediment to the Arctic Ocean are dominated by river discharge, coastal erosion,
199 current transport, turbidites and slumping, while aeolian transport plays only a minor
200 role (*Stein, 2008*). The bulk of the sediment deposited in the central Arctic Ocean is
201 transported by sea ice or icebergs, whose trajectories are governed by the two major
202 circulation patterns, the Beaufort Gyre and the Transpolar Drift. The mineralogical
203 composition of the sediment that enters the Arctic is controlled by the geology of the
204 surrounding land masses, with the Canadian Arctic and Greenland containing
205 abundant carbonate rocks, while widespread basaltic rocks on the Eurasian side
206 results in sediment with abundant heavy minerals (*Stein, 2008*). It has long been
207 recognized that these differences in bedrocks results in clearly distinguishable mineral
208 assemblages (*Lapina, 1965; Levitan et al., 1999*) or chemical composition (*Rachold et*
209 *al., 1999*) in the IRD, reflecting the origin of the sediment. These differences also
210 result in characteristic distributions of clay minerals in the Arctic region, providing a
211 powerful tool to tie Arctic sediments to their source regions (*Wahsner et al., 1999;*
212 *Vogt, 1997*).

213 One of the most conspicuous features of late Quaternary Arctic sediments is
214 the cyclical occurrence of brownish, Mn-rich layers observed in sediment cores from
215 all over the deep Arctic Ocean (*Clark et al., 1980; Jakobsson et al., 2000; Polyak,*
216 *1986; Poore et al., 1993*). Biostratigraphic dating and the cooccurrence with enhanced
217 levels of benthic and planktonic foraminifera show that these layers formed during
218 interglacial conditions (*Jakobsson et al., 2000; Löwemark et al., 2008; Poore et al.,*
219 *1993*) (*O'Regan et al., 2008; O'Regan et al., 2010*). However, the mechanism for the
220 formation of these layers remains debated, and several different physical and chemical
221 processes have been invoked (*Macdonald and Gobeil, 2011; März et al., 2011*). In
222 most modern sediments, Mn-rich layers typically form close to the sediment surface

223 where Mn mobilized by the degradation of organic matter encounters downwards
224 diffusing oxygen from the bottom waters, thereby marking the position of the redox
225 boundary (e.g., Burdige, 2006; Froehlich et al., 1979). It has therefore been suggested
226 that the Mn observed in Arctic sediments would largely represent diagenetic processes
227 (Li et al., 1969). However, the recurrent down-core and near synchronous occurrence
228 of Mn enrichment, bioturbation, and calcareous micro- and nanofossils strongly
229 suggest that the Mn enrichment formed as a direct response to environmental
230 conditions in the circum Arctic region. Changes in deep water ventilation and the
231 related dissolution or precipitation of Mn, and variations in Mn input from the
232 terrestrial realm are the two main mechanisms that have been discussed (e.g.,
233 Jakobsson et al., 2000; Löwemark et al., 2008; Macdonald and Gobeil, 2011;
234 Mashiotta et al., 1999). That the dramatic changes in basin geometry and sea ice cover
235 related to glacial-interglacial climatic swings also greatly affect Arctic deep water
236 circulation is obvious (Haley et al., 2008; Jakobsson et al., 2010; Poirier et al., 2012).
237 However, in order to remove Mn from the sediment the bottom waters must become
238 depleted of oxygen, which would require a steady flux of labile organic matter to the
239 sea floor. As primary productivity reaches absolute minima during glacial periods, a
240 depletion of bottom water oxygen seems unlikely. Further arguments against oxygen
241 depletion of Arctic bottom waters comes from the presence of benthic ostracodes
242 which persist also in glacial intervals, evidencing at least minimal oxygen levels in the
243 deep basins (Poirier et al., 2012). An active removal of Mn from the sediment during
244 glacial intervals was also deemed unlikely when the ratios of Mn to Al were studied.
245 März et al (2011) demonstrated that glacial Mn/Al ratios actually lie close to average
246 shale values, strongly suggesting that no Mn was dissolved from the sediments.

247 Instead, Maconald and Gobeil (Macdonald and Gobeil, 2011) demonstrated
248 through Mn budget calculations that changes in coastal erosion and riverine input can
249 explain the large variability in Mn observed. During interglacials, the high sea level
250 promoted intense coastal erosion and remobilization of Mn on the shelves at the same
251 time as the Mn-rich circum-Arctic rivers flew unhindered into the Arctic Ocean. In
252 contrast, during glacial periods, the low sea level hindered coastal erosion while the
253 Arctic rivers were blocked by the Eurasian ice sheet, both processes limiting the
254 supply of Mn to the Arctic Ocean. Maconald and Gobeil (Macdonald and Gobeil,
255 2011) did not include hydrothermal input into their budget calculations as data is still
256 exceedingly scarce, but several lines of evidence speak against a hydrothermal origin
257 of the Mn enriched layers. First, modern Mn concentrations are highest in near surface
258 waters and show a clear correlation with salinity minima (Middag et al., 2011),
259 strongly indicating a riverine or shelf origin rather than a hydrothermal. Second, the
260 Mn plume observed in the water column over the Gakkel Ridge shows a maximum
261 between 2000 and 4000 m, and very low values above 2000 m (Middag et al., 2011).
262 Since Mn enriched layers are ubiquitous in sediments retrieved at water depths even
263 shallower than 1000 m (Jakobsson et al., 2000; Macdonald and Gobeil, 2011),
264 hydrothermal sources are considered unlikely. Third, Mn concentrations in the water
265 column show exponentially decreasing values with distance from the ridge (Middag et
266 al., 2011), making a basin wide influence unlikely although locally the effect of
267 hydrothermal input may be significant. Fourth, there is no reason to assume any
268 significant glacial-interglacial variability in the hydrothermal input of Mn.

269 **3 Material and methods**

270 The core material used in this study was obtained during four expeditions to
271 the Arctic Ocean using the ice breakers Ymer (YMER 80) and Oden (Arctic Ocean

272 96, LOMROG-07, LOMROG-09) as research platforms. The 12 piston and gravity
273 cores vary in length between 198 and 765 cm (Table 1) and consist primarily of ice
274 rafted debris (IRD) and pelagic muds. The sampled area spans from the Makarov
275 Basin to the Yermak Plateau via the central Lomonosov Ridge, the Lomonosov Ridge
276 off Greenland, the Gakkel Ridge, and the Morris Jesup Rise (Fig. 1).

277 Physical properties were analyzed onboard using a GEOTEK Multi Sensor
278 Core Logger during LOMROG-07 and LOMROG-09, while AO96-12pc was
279 measured at Stockholm University. Variations in Mn distribution were determined
280 directly on split cores using the Itrax XRF-core scanner (cf. Croudace et al., 2006) at
281 Stockholm University. The resolution used for XRF-scanning ranged from 0.2 to 5
282 mm. Exposure times were adjusted to the individual cores and typically vary between
283 5 and 20 seconds. X-ray radiographs were produced by cutting thin slabs of sediment
284 from the cores using plastic boxes approximately 6 mm thick (cf. Löwemark and
285 Werner, 2001; Werner, 1967). The slabs were then analyzed (55kV/3mA, 3 minutes)
286 at the X-ray facility in the Faculty of Geosciences at the University of Bremen.

287 On a limited number of the sediment slabs used for X-ray radiography from
288 AO96-14GC, detailed studies were performed using microscope and scanning
289 electron microscope. In intervals containing denser, horizontal layers in the
290 radiographs, the corresponding sediment slabs were meticulously subsampled and
291 the sediment studied under microscope to identify the aggregates causing this
292 layering. A number of grains were selected and analyzed with SEM and electron
293 microprobe (Philips Analytical XL-30- *ESEM-FEG*) to study the chemical
294 composition of individual grains.

295 4 Results

296 4.1 Trace fossils and spatial differences in their distribution

297 The trace fossil fauna is generally sparse with only a few ichnospecies or
298 ichnogenera present. In most sediment cores *Planolites*-like structures were observed
299 and many cores contain small, mineralized burrows similar to *Trichichnus*. The trace
300 fossils *Chondrites*, *Phycosiphon*, and *Scolicia* occur sporadically. In two of the cores
301 isolated occurrences of *Zoophycos* were noted. *Nereites*-like traces were abundant in
302 core LOMROG09-PC10, but occurred only sporadically in a few other cores. On
303 several occasions, biodeformational structures (cf. Bromley, 1996) without any
304 identifiable trace fossils were observed. Basic trace fossil morphology and ethology is
305 described in Table 2.

306 The abundance of trace fossils in the cores shows a clear spatial pattern. The
307 cores from the central Lomonosov Ridge, the Makarov Basin and the Yermak Plateau
308 display stronger bioturbation with more diverse ichnofauna than those from the
309 Lomonosov Ridge off Greenland, Morris Jesup Rise and the Gakkel Ridge (Fig. 2). In
310 cores from the Lomonosov Ridge off Greenland, a few *Planolites*-like traces were
311 found in the top sections and a few mineralized tubes scattered in the lower parts of
312 the cores. A common feature in the cores from the Lomonosov Ridge off Greenland,
313 the Morris Jesup Rise, and the Gakkel Ridge is the high content of IRD seen in the
314 radiographs. The core from the Gakkel Ridge is almost completely devoid of biogenic
315 structures. This core was taken on the flank towards the Amundsen Basin, and the
316 sediment fabric is almost totally dominated by primary sediment structures indicating
317 that it could be a contourite body. With the exception of the Gakkel Ridge, areas with
318 few trace fossils correspond to the regions experiencing the most severe ice-

319 conditions, today characterized by nearly complete ice-coverage even during summer
320 (Comiso et al., 2008).

321 4.2 *Chronostratigraphy and sedimentation rate variability*

322 To allow comparisons between down-core variations in trace fossil
323 composition and paleoclimatic variations, we relied on published age models and
324 stratigraphic correlations between relatively closely spaced cores. Abundances of
325 calcareous nanno- and microfossils were previously used to locate marine isotope
326 stages (MIS) 5, 3 and 1 on the Lomonosov Ridge (Backman et al., 2009; Spielhagen
327 et al., 2004), Lomonosov Ridge off Greenland (Jakobsson et al., 2010), Morris Jessup
328 Rise (Hanslik et al., in press; Jakobsson et al., 2010) and the Yermak Plateau
329 (Dowdeswell et al, 2010).

330 Only some of the cores from the central Lomonosov Ridge have tentative age
331 models that extend beyond MIS 6. These are based on the cyclostratigraphic analysis
332 of the ACEX record (O'Regan et al., 2008), and stratigraphic correlations to near-by
333 sediments using bulk density and XRF-derived Mn profiles (Fig.3).

334 A number of cores collected from the Lomonosov Ridge (LOMROG09-PC08,
335 LOMROG09-PC05, LOMROG09-PC10, AO96-14GC, AO96-16-GC) and Gakkel
336 Ridge (AO96-B13-1PC) either lack the required physical property data for
337 establishing stratigraphic correlations, or display a more complex downhole bulk
338 density profile that precludes straightforward alignment with the ACEX record (Fig.
339 4). To provide tentative age control, we rely on a distinct dark-grey layer as a
340 common tie point to other cores from the region. It is characterized by a sharp lower
341 boundary, enhanced IRD content, prominent variations in elements such as Fe and Ti,
342 and often bounded by a sharp shift in Mn content. The sharp lower boundary and the
343 distinct sedimentary and geochemical features of this layer suggest synchronous

344 deposition over much of the Eurasian Basin. On the central Lomonosov Ridge, the
345 grey-layer is found near the base of a coarse grained diamicton deposited around the
346 MIS 3/4 boundary (Spielhagen et al., 2004). In some cores, a second grey layer is
347 found near the base of a second prominent coarse-grained diamicton associated with
348 MIS6 (Fig. 4). Below these grey layers and the associated Mn minima, MIS 5 can
349 usually be identified through the correlation of a triplet of Mn peaks (Fig. 4). We do
350 not attempt to extend the age model further back than MIS 5 in these records.

351 Sedimentation rates in the studied cores range from 0.2 to 2.1 cm/ky with
352 typical values around 0.5-1 cm/ky (Table 3), which is in agreement with what has
353 been observed in earlier studies (Backman et al., 2004; Sellén et al., 2008; Spielhagen
354 et al., 2004). The cores from the central Lomonosov Ridge have higher average
355 sedimentation rates compared to the cores from the Makarov Basin, Morris Jesup
356 Rise, and the Lomonosov Ridge off Greenland, where sedimentation rates are
357 generally below 1 cm/ky. The Gakkel Ridge is somewhere intermediate with 1 cm/ky,
358 but the age model lacks any firm age control points. The highest sedimentation rates
359 were observed on the Yermak Plateau (2.0cm/ky) and in the top section of
360 LOMROG09-PC08 from the crest of the Lomonosov Ridge (2.1cm/ky).

361 A seemingly general difference in sedimentation rates was observed between
362 gravity cores and piston cores, the later having higher sedimentation rates. It is
363 uncertain whether this is due to sediment shortening, which is often observed in
364 gravity cores (Emery and Hülsemann, 1964; Löwemark et al., 2006), or if it represents
365 an actual difference in sedimentation rate between the sites. Sedimentation rates in the
366 younger interval, MIS 1 to 7, are considerably higher than in the older intervals,
367 where sedimentation rates are often half or less. Explanations for this observation
368 include a) the expected downhole decrease in sediment porosity due to mechanical

369 compaction, which is especially pronounced in the upper few meters of sediments,
370 and b) the occurrence of relatively thick sandy intervals previously described as
371 diamictons (Svindland and Vorren, 2002) that occur during late Quaternary
372 glacial/stadial stages (MIS 6, 5b, 5/4 and 3/4) in the central Lomonosov Ridge cores
373 (Spielhagen et al., 2004).

374 4.3 Temporal variations in trace fossils and bioturbation

375 4.3.1 Lomonosov Ridge off Greenland, Morris Jesup Rise, and the Yermak Plateau

376 In the cores from the Lomonosov Ridge off Greenland, the ichnofauna is
377 sparse consisting primarily of *Planolites*-like burrows concentrated to the brown
378 layers in MIS 1 and 5 (Fig. 5). In the lower part, below MIS 5, only occasional,
379 mineralized *Trichichnus* and *Chondrites* were found. Both cores contain large
380 amounts of IRD, and in the lower part conspicuous bands of closely spaced,
381 horizontal, thin layers are visible in the X-ray radiographs. High-resolution XRF-
382 scanner measurements clearly show that these thin and dense layers are enriched in
383 Mn. The core from the Morris Jesup Rise was taken in the centre of an iceberg-scour
384 (Jakobsson et al., 2010) and the sediments below the erosional surface at about 128
385 cm are likely pre-Quaternary. Some *Planolites*-like traces were observed in MIS 5
386 while glacial intervals are free of trace fossils. The core contains abundant IRD,
387 although not as much as the cores from the Lomonosov Ridge off Greenland. Just
388 below MIS 1, which consists of homogenous, IRD-rich, non-bioturbated sediment, a
389 number of horizontal, Mn-rich bands similar to the ones observed in the cores on the
390 Lomonosov Ridge off Greenland are seen.

391 The core from the Yermak Plateau differs markedly from the cores on the
392 Lomonosov Ridge off Greenland and the Morris Jesup Rise (Fig. 5). Sedimentation

393 rates are almost an order of magnitude higher here and bioturbation is much more
394 intense and diverse with *Planolites*, *Phycosiphon*, and possibly *Trichichnus* in the
395 Holocene part, and biodeformational structures in the last glacial interval. MIS 3 is
396 characterized by enhanced levels of IRD and an ichnofauna dominated by *Planolites*
397 and *Trichichnus*. Interestingly, an interval in MIS 3 characterized by brownish colour
398 and high Mn content is totally barren of trace fossils but contains extreme amounts of
399 IRD.

400 4.3.2 Central Lomonosov Ridge

401 The cores from the central Lomonosov Ridge display a more intense
402 bioturbation and diverse ichnofauna consisting of large numbers of *Planolites*-like
403 burrows, occasional *Phycosiphon*, numerous mineralized small tubes belonging to
404 *Chondrites* and *Trichichnus*, abundant *Nereites* in certain intervals, and a few
405 occurrences of *Zoophycos* in the deeper cores. In all cores there is a clear overall
406 correspondence between bioturbation intensity and intervals with brown, mottled
407 sediments rich in Mn (Figs. 6 & 7). There is also a more diverse ichnofauna in the
408 deeper cores from the slope and intrabasin as compared to the cores from the ridge
409 crest (Table 3). The ichnofauna in the cores from deeper sites contain more complex
410 traces such as *Nereites* and *Zoophycos*.

411 4.3.3 Makarov Basin and the Gakkel Ridge

412 The two cores from the basins, LOMROG09-GC03 (3814 m water depth) from the
413 Makarov Basin and AO96-B13 (2079 m water depth) from the Gakkel Ridge, display
414 diametrically opposed patterns although both are situated in relatively deep waters
415 away from the Lomonosov Ridge. In the Makarov Basin the ichnofauna is fairly
416 diverse with four different ichnospecies: *Chondrites*, *Nereites*, *Phycosiphon*, and

417 *Planolites*. In contrast, on the Gakkel Ridge only uncertain *Planolites*-like traces were
418 observed. In the Makarov Basin the trace fossils display the same pattern as on the
419 ridge crest, closely following variations in Mn (Fig. 7).

420 4.4 *Individual trace fossils and their interpretation*

421 The sparse occurrence of trace fossils and the low diversity make it difficult to
422 determine the ichnofacies of the studied cores. However, the presence of *Zoophycos*
423 and *Nereites* together with the generally deep bathymetric position of the cores
424 suggest either *Zoophycos*- or *Nereites*-ichnofacies (cf. Seilacher, 1964). The low
425 ichnodiversity also makes it irrelevant to use terms such as ichnocoenosis or
426 ichnoassemblages to describe the ichnofabric, which is almost always totally
427 dominated by one or two ichnospecies. The low ichnodiversity also limits the
428 development of tiering of different trace fossils into different vertical zones in the
429 sediment. There is little evidence for any deep-reaching burrows apart from
430 mineralized, thin tubes such as *Trichichnus* and *Chondrites* which are seen to cross-
431 cut the other trace fossils. A thorough look at the individual trace fossil species
432 reveals additional information about the depositional settings and the variations in
433 environmental parameters.

434 4.4.1 *Chondrites*

435 *Chondrites* occurs sporadically in 9 out of 12 cores and is usually found in or
436 just below sediments with enhanced Mn levels. It often occurs together with
437 *Trichichnus* or *Planolites*. Together with *Trichichnus* it is usually the trace fossil
438 reaching deepest into the sediment, cross-cutting the other traces.

439 *Chondrites* are believed to represent a chemosymbiotic behavior where the
440 producing organism utilizes the redox gradient between anoxic pore waters and

441 oxic/dysoxic bottom waters to cultivate microbes for food or energy (Fu, 1991;
442 McBride and Picard, 1991; Seilacher, 1990). The burrow producers consequently
443 have a high tolerance for low-oxygen pore-water conditions. Massive occurrences of
444 *Chondrites* have been interpreted to be indicative of poorly oxygenated bottom waters
445 creating favourable conditions for an opportunistic colonization of a niche
446 inaccessible to other burrowers (Ekdale, 1985; Ekdale and Mason, 1988). In contrast,
447 where deep reaching *Chondrites* occupy the deepest tiers, it represents an equilibrium
448 behaviour. For example, on the Iceland-Færø ridge, where bottom water conditions on
449 the northern side are sluggish, the ichnofauna is dominated by dense occurrences of
450 *Chondrites*, while the southern slope where bottom water circulation is more
451 vigorous, the ichnofauna is characterized by a diverse set of trace fossils (Fu and
452 Werner, 1994). Similarly, on the Portuguese continental slope massive occurrences of
453 *Chondrites* are found in intervals characterized by sluggish bottom-water currents and
454 the deposition of organic-rich sediments. Conversely, intervals where TOC content
455 and grain size indicated well-oxygenated conditions were characterized by *Chondrites*
456 at deep tiers below the other traces indicating equilibrium positions (Löwemark,
457 2003).

458 Accordingly, in the Arctic Ocean, the sparse occurrence of *Chondrites* rather
459 suggest stable conditions with oxygenated bottom waters where *Chondrites* occupies
460 the deepest tier and therefore avoids obliteration by larger burrowers (cf. Savrda and
461 Bottjer, 1986). In most cores they are primarily found in the interglacial sections
462 where they inhabit a deep tier cross-cutting the few other traces present. This suggests
463 an equilibrium behavior where the producers colonize the deeper parts of the sediment
464 whenever the food flux is rich enough.

465 4.4.2 *Nereites*

466 *Nereites*, or *Nereites*-like traces, only occur in three cores. In LOMROG09-
467 GC03 from the Makarov Basin, it is found in the interstadial/glacial interval around
468 MIS 3 and during an interglacial interval tentatively associated with MIS 11. In
469 LOMROG09-PC05 from the intrabasin only one uncertain observation at the top of
470 what is believed to be the interglacial MIS 5 was made. In contrast, the third core
471 containing *Nereites*, LOMROG09-PC10 from the slope of the Lomonosov Ridge,
472 shows massive occurrences of *Nereites* in all interglacials before MIS 5, but no
473 *Nereites* in stage 5 or younger sediment. These three cores were taken at water depths
474 exceeding 2 km. *Nereites* is generally cross-cut by other traces suggesting a shallow
475 tier.

476 The winding horizontal trace fossil *Nereites* is so common in fossil strata from
477 turbiditic settings that Seilacher (1967) named one of his archetypical ichnofacies
478 after it. Later the *Nereites* ichnofacies was expanded to encompass bathyal to abyssal
479 settings with slow stable sedimentation and well oxygenated conditions (Frey and
480 Pemberton, 1984).

481 In fossil strata, *Nereites* is usually the uppermost tier and is almost exclusively
482 preserved as horizontal, winding traces (Seilacher, 1962). The preservation is often
483 linked to frequent turbidites preventing a subsequent obliteration by later, deeper
484 burrowers. The shallow tier makes observations on *Nereites* in sediment cores rare as
485 top sediments are usually too soupy to allow the preparation of X-ray radiographs,
486 and in the part of the core under the mixed layer, deeper penetrating traces have
487 destroyed *Nereites*. However, in a suite of 19 box cores taken in the South China Sea,
488 detailed studies show that the trace fossil starts almost vertical and penetrates down to
489 just above the redox boundary where it levels out and becomes almost horizontal,

490 keeping a constant distance of 1-2 cm to the redox boundary (Wetzel, 2002). Wetzel
491 (2002) suggested that the producers fed on bacteria which thrived on organic matter
492 available at the boundary between reducing and oxidizing conditions. In the Arctic
493 Ocean material, *Nereites* only occurs in settings deeper than 2 km and it is only on the
494 Amundsen basin slope of the Lomonosov Ridge (LOMROG09-PC10) that *Nereites*
495 occurs abundantly. This abundant occurrence in presumably interglacial intervals
496 indicates fairly high food fluxes, well-oxygenated bottom waters, and a redox
497 boundary that is situated some 3 to 9 cm into the sediment (cf. Wetzel, 2002). The
498 disappearance of *Nereites* in glacial intervals with low Mn content could suggest
499 either decreased food flux or decreased bottom water oxygenation or a combination of
500 both.

501 Today the Eurasian flank of the Lomonosov Ridge experiences enhanced food
502 flux because of lateral advection by the Arctic Intermediate Water. Deubel (2000)
503 indeed found lateral sediment transport along the Lomonosov Ridge to be an
504 important mechanism for the distribution of food and consequently for the distribution
505 of benthos. In this context it is therefore interesting to note a distinct change in the
506 ichnofauna from abundant *Nereites* below MIS 5 to no *Nereites* in MIS 5 and above,
507 in core LOMROG09-PC10. This could be indicative of a major reorganization in the
508 Arctic deep-water circulation around the boundary between MIS 6 and 5. The nature
509 of this oceanographic change remains elusive, however.

510 4.4.3 *Phycosiphon*

511 *Phycosiphon* was only found in one short interval in the core from the Yermak
512 Plateau where it is situated between a *Planolites* dominated interval below, and
513 *Trichichnus* burrows above. *Phycosiphon* is the trace of a deposit feeder and is
514 interpreted to be an indicator for oxic to dysoxic conditions (Ekdale and Mason,

515 1988). Studies of *Phycosiphon* from the Indian Ocean (Wetzel and Wijayananda,
516 1990) and the Iceland-Faroe Ridge (Fu and Werner, 1994) both show a shallow tier
517 position and a preference for well oxygenated conditions. The position above an
518 interval with *Planolites*, which require high oxygen levels, but below an interval with
519 *Trichichnus*, which tolerate low oxygen levels, therefore could indicate a trend of
520 decreasing bottom water oxygenation in the upper part of the Holocene section of this
521 core.

522 4.4.4 *Planolites*

523 *Planolites*, or rather *Planolites*-like traces were observed in all cores. The
524 occurrences of *Planolites* show a close correspondence to brownish layers and
525 increased Mn content.

526 *Planolites* is a trace left by a wide range of deposit-feeding organisms that
527 require rather well-oxygenated conditions. As larger organisms require more oxygen
528 for their metabolism than small ones (Savrda and Bottjer, 1989), the size of *Planolites*
529 has been used as an indicator for variations in bottom water oxygen levels (Tyzka,
530 1994; Wetzel, 1991). Studies of trace fossils from the continental slope off Portugal
531 (Löwemark et al., 2004) and the Iceland-Faroe Ridge (Fu and Werner, 1994) show
532 that in sediments deposited under sluggish, poorly oxygenated bottom waters, only
533 few and small *Planolites* were observed and the ichnofauna was dominated by traces
534 such as *Chondrites*. In contrast, where bottom water ventilation was vigorous the
535 ichnofauna contained numerous, large *Planolites* and other traces such as *Scolicia* that
536 are known to thrive under well-oxygenated conditions.

537 The strong correspondence between *Planolites* and Mn-enrichment therefore
538 suggest that bottom waters were fairly well oxygenated during the interglacial
539 intervals when Mn was precipitated.

540 4.4.5 *Scolicia*

541 *Scolicia*-like traces were observed in core LOMROG09-PC08 and AO9616-
542 2GC from the crest of the Lomonosov Ridge, and in LOMROG09-PC10 from the
543 slope of the Lomonosov Ridge. *Scolicia* is a deposit feeding trace produced by
544 irregular sea urchins, and the producers have a profound preference for well-
545 oxygenated, silty sediment (Fu and Werner, 2000). The occurrence together with
546 numerous oxygen demanding traces such as *Planolites* or *Nereites*, in sediment with
547 low IRD-content consequently agrees well with the stratigraphic positions in
548 interstadial MIS 3 when more food, less IRD, and better oxygenated bottom waters
549 would be expected.

550 4.4.6 *Trichichnus*

551 *Trichichnus* and similar trace fossils with cemented tubes occur in about half
552 of the studied cores, often the burrows are mineralized, presumably by the formation
553 of Rhodochrosite (cf. Eriksson et al., submitted; Taldenkova et al., 2010). In cores
554 with weak bioturbation the *Trichichnus* tubes tend to be concentrated to Mn-rich
555 intervals while in more strongly bioturbated cores with abundant trace fossils the
556 *Trichichnus* tend to occupy the Mn-poor intervals between the interglacial intervals.
557 This pattern is especially apparent in cores LOMROG09-PC08 and LOMROG09-
558 PC10 (Fig. 6). On the Vøring Plateau off Norway, sipunculid worms were shown to
559 produce modern *Trichichnus* (Romero-Wetzel, 1987), and the trace has been
560 interpreted to represent a chemosymbiotic behavior where the organism utilizes the
561 redox gradient much in the same way as the producers of *Chondrites* (McBride and
562 Picard, 1991). The occurrence of *Trichichnus* between strongly bioturbated intervals
563 therefore may be the opportunistic response to a niche that cannot be accessed by
564 other burrowers because of decreased food flux during glacials. The decrease in input

565 of organic carbon would result in a downwards shift in the redox boundary, forcing
566 the trace makers to construct the long vertical burrows observed in the glacial
567 sediment. Deep below the sediment surface they then utilize microbes to access the
568 refractory carbon available in the sediment.

569 The fact that the glacial intervals between the *Nereites*-dominated sections are
570 characterized by numerous *Trichichnus* and *Chondrites* burrows, whose producers are
571 believed to utilize the redox gradient between dysoxic pore waters and oxic bottom
572 waters (Blanpied and Bellaiche, 1981; Löwemark, 2003; McBride and Picard, 1991),
573 suggest that Arctic bottom water oxygenation levels remained oxic even during
574 glacial intervals. This interpretation is further supported by the presence of ostracodes
575 in glacial intervals (Poirier et al., 2012), which require oxygenated waters to survive.

576 4.4.7 *Zoophycos*

577 *Zoophycos* spreiten occur in conjunction with interglacial intervals in the core
578 from the intrabasin, and in the core from the slope towards the Amundsen Basin. Both
579 single horizontal spreiten and inclined spreiten diverging from a central axis were
580 observed. However, neither the central shaft nor open marginal tubes were found in
581 the studied material. None of the spreiten show the typical minor lamellae found in
582 many types of *Zoophycos*, but are homogeneous.

583 *Zoophycos* is actually a diverse group of complex spreiten structures for which a
584 plethora of ethological explanations has been put forward (cf. Bromley, 1991; Fu and
585 Werner, 1995; Gong et al., 2008; Kotake, 1997; Olivero, 1995). For the *Zoophycos*
586 found in Quaternary deep marine settings, however, it has been shown that the trace
587 likely is a cache where food is squirreled away for use when food becomes less
588 plentiful (Löwemark, 2012; Löwemark and Schäfer, 2003).

589 Thus, although the presence of *Zoophycos* is sparse, it can be viewed as an
590 adaptation by the benthos to the strong seasonality in food flux (Arrigo et al., 2008)
591 observed in the Arctic Ocean today. It has been postulated that this kind of adaption
592 would be expected in the Arctic Ocean because of the extreme difference in food flux
593 between summer and winter seasons (Van Averbek et al., 1997). During Arctic
594 summers the primary productivity is extremely high due to the permanent sun-light
595 and high nutrient concentrations. Conversely, during Arctic winters, the complete ice
596 coverage and total darkness results in extremely low food fluxes to the sea floor. The
597 *Zoophycos* producers would collect food during the rich summer months and store it
598 deep in the sediment to be used during the poor winter months (Löwemark, 2012). In
599 contrast, during glacial intervals the ice cover may have neared 100% also during in
600 summers, with primary productivity limited all year round, resulting in unfavourable
601 conditions even for *Zoophycos*.

602 4.5. Horizontal bands of Mn

603 In four of the studied cores, distinct thin, horizontal bands were observed in
604 the radiographs, and are expressed as higher Mn values in the XRF-scanner data (Fig.
605 8). These bands have the appearance of horizontal layers that are lighter, thus more
606 dense, than surrounding sediment, or as layers of frost-like crystals that extend in a
607 dendritic fashion downwards and therefore must have formed *in situ*. This kind of
608 horizontal bands were found in two cores from the Lomonosov Ridge off Greenland,
609 on the Morris Jesup Rise and in one core from the crest of the central Lomonosov
610 Ridge. Only in core LOMROG07-GC10 on Morris Jesup Rise can the layers be dated
611 with any certainty as they occur between MIS 1 and a dark grey layer likely deposited
612 at the MIS 3-4 boundary. In the cores from the Lomonosov Ridge off Greenland they
613 occur in what could be MIS 5 and MIS 7, but here age control is weak. In AO96-

614 14GC from the central Lomonosov Ridge the horizontal bands are situated between
615 MIS 5 and MIS 7. The bands occur in sediment that does not show any sign of
616 bioturbation and in three of the intervals the sediment does not display the typical
617 brownish colour associated with Mn-rich sediments despite the high Mn content.
618 High-resolution XRF-scanning was performed on a selected number of sediment slabs
619 used for X-ray radiography in core AO96-14GC. Subsamples taken in the interval
620 containing the frost-like crystals show that the grains consist of small blackish
621 aggregates of quartz grains cemented and draped by a Mn-rich matrix (Fig. 9).

622 **5 Discussion**

623 *5.1 Spatial variability in bioturbation and trace fossils*

624 The difference in abundance and diversity between the individual regions,
625 with sparse ichnofauna on the Lomonosov Ridge off Greenland and on the Morris
626 Jesup Rise, and relatively abundant and diverse ichnofauna in the central Arctic, is in
627 agreement with the spatial variability of several environmental parameters. For one,
628 the cores from the sites north of Greenland contain considerably more IRD than the
629 sites from the central Arctic. Although sediment composition and substrate
630 consistency exert a major control on animal behavior and burrow construction
631 (Bromley, 1996), studies from the Greenland Sea suggest that grain-size variations
632 and IRD has only minor influence on benthic biomass and diversity (Schnack, 1998).
633 In contrast, a recent review showed that grain size variation, bottom-water
634 oxygenation, food flux and bottom-current intensity are the main factors controlling
635 species abundance and diversity (Levin et al., 2001). These are also the factors
636 identified as the most important ones controlling variations in trace fossils (Wetzel,
637 1991). In the area north of Greenland food flux is low because of the tough sea-ice

638 conditions (Comiso and Nishio, 2008) and the sediment has been impacted by drifting
639 icebergs at least during MIS 6 (Jakobsson et al., 2010). In sediments on the West
640 Antarctic Peninsula increased iceberg scouring was shown to strongly increase the
641 mortality of benthic organisms (Barnes and Souster, 2011). It remains unclear,
642 however, if iceberg scouring during glacial periods would have any impact on the
643 interglacial benthic fauna. Nevertheless, a combination of factors unfavourable for
644 benthic organisms coincides and results in a sparse ichnofauna and weak bioturbation
645 in this region. In the central Arctic, summer sea-ice conditions are less severe
646 resulting in stronger food flux, and the sediment contain less IRD, creating more
647 favourable conditions for benthic life.

648 The most intense bioturbation was found in the core from the Yermak Plateau
649 while the weakest bioturbation was found on the Gakkel Ridge, with the central
650 Lomonosov Ridge taking a middle position. This agrees with observations on the
651 modern distribution of benthos in the Eurasian Basin. The biomass on the Morris
652 Jesup Rise and on Gakkel Ridge showed low values similar to the deep basins while
653 the Lomonosov Ridge and the Yermak Plateau displayed higher biomass (Kröncke,
654 1994; Kröncke, 1998). It is therefore reasonable to assume that the factors controlling
655 the benthos today should also be reflected in the down-core variations in bioturbation
656 intensity and trace fossil composition.

657 5.2 *Temporal variability in bioturbation and trace fossils*

658 That food is an important factor controlling bioturbation is corroborated by the
659 temporal variability in trace fossil abundance and diversity. The cores from the central
660 Arctic clearly show a strong increase in bioturbation during interglacial intervals
661 when decreased sea-ice and more open-water conditions led to enhanced primary
662 productivity. In the area north of Greenland this connection is not as distinct as there

663 is only a sparse ichnofauna to begin with, but the few trace fossils that do occur are
664 concentrated to interglacial intervals. The hypothesis that brownish, Mn-rich intervals
665 were deposited under interglacial conditions when biological activity at the sea-floor
666 was stronger therefore seems to be validated. However, while the Mn cycles
667 representing glacial-interglacial changes are ubiquitous in both the Eurasian and
668 Amerasian Basins (Clark, 1970; März et al., 2011; Phillips and Grantz, 1997), the
669 response in bioturbation appears more spatially limited and is likely a consequence of
670 variations in perennial sea-ice cover.

671 From the observations on trace fossil distribution and Mn cycles in
672 combination with recent work on the Arctic Mn-budget (Macdonald and Gobeil,
673 2011) and detailed studies on the geochemistry of the Mn-rich layers (März et al.,
674 2011), a conceptual model for the formation of the Mn layers may be drafted.

675 During interglacial periods (Fig. 10), when ice sheet are restricted to
676 Greenland and high sea levels flood the huge shelf areas, large amounts of Mn enters
677 the Arctic Ocean from riverine input and coastal erosion. This Mn is initially
678 deposited on the shelves where it undergoes a number of redox cycles before it enters
679 the deep ocean where the low organic carbon levels allow preservation and
680 incorporation into the geological archive (Macdonald and Gobeil, 2011). The
681 enhanced primary productivity caused by increased open waters led to an increased
682 food flux, resulting in a more intense bioturbation. As organic particles are known to
683 effectively scavenge Mn from the water column (Johnson et al., 1996; Martin and
684 Knauer, 1980), this process also most likely contributed substantially to the enhanced
685 Mn levels observed in interglacial sediments. The bio-irrigation of the sediment
686 caused by the mixing activities of the benthic organisms control the depth of the redox
687 boundary, and therefore also ensure a close to synchronous position of increased Mn

688 levels and increased bioturbational structures in the sediment. Post sedimentary Mn
689 diagenesis, although locally of large importance, play an insignificant role in the
690 formation of the interglacial Mn maxima

691 During glacial periods, characterized by the enormous ice sheet and drastically
692 lowered sea level, the input of Mn by rivers and coastal erosion was limited to a
693 minimum (Macdonald and Gobeil, 2011), while the perennial ice pack that covered
694 the remaining Arctic basin prohibited or at least strongly limited primary productivity
695 even during the summer months, and as a consequence the food flux to the sea floor
696 also decreased, resulting in a sparse benthic fauna. A decreased flux of organic
697 particles through the water column would also drastically reduce scavenging of Mn.
698 The remaining benthic organism resorted to the use of refractory carbon deep in the
699 sediment which they accessed with the help of chemosymbiotic strategies involving
700 microbes that took advantage of the redox gradient between pore waters and bottom
701 waters. The resulting sediments are characterized by a sparse ichnofauna dominated
702 by *Chondrites* and *Trichichnus*, Mn levels close to lithogenic background levels and
703 few or no planktic foraminifera.

704 *5.3. The horizontal bands of Mn and diagenetic alteration of Mn-distributio*

705 The comparison of X-ray radiographs, XRF-scanner data of down-core Mn
706 variations, and lithological appearance of the sediment reveal two deviations from the
707 general pattern of strong bioturbation in the Mn-rich sediments, and weak
708 bioturbation in sediments with low Mn content. First, some intervals display vigorous
709 bioturbation although XRF-scan data show minima in Mn, and second, in other
710 intervals strong maxima in Mn occur in sediments completely devoid of trace fossils.
711 The first case is clearly related to an IRD-rich grey layer often found close to the
712 boundary between MIS 3 and 4, but in some instances also near MIS 6. Below these

713 grey layers, the Mn content drops to levels close to zero, but the sediment still
714 contains numerous trace fossils indicating interglacial/interstadial conditions. For
715 example, in AO96-14GC from the central Lomonosov Ridge the sediment below the
716 layer is vigorously bioturbated by *Planolites*-like structures but the Mn content is
717 close to zero. Just below the boundary between the overlying IRD-rich layer and the
718 bioturbated, fine grained sediment, a sub-vertical trace fossil with the characteristics
719 of an escape trace can be seen (Fig. 11). The sharp boundary marking the shift from
720 fine-grained sediments to IRD-rich sediments and the escape trace suggest that this
721 layer was deposited extremely rapidly. This event-like layer would act as a lid
722 shutting off downwards diffusion of oxygen into the sediment. As pore-water oxygen
723 in the underlying sediment is consumed, pore water would become anoxic and the Mn
724 originally present would dissolve and diffuse and re-precipitate in overlying regions.
725 This is seen as a sharp Mn peaks just above the grey, Mn-poor intervals (Fig. 6).
726 Thus, the Mn originally deposited during interglacial conditions has disappeared, but
727 the trace fossils remain as witnesses. The extremely low levels of Mn underneath the
728 grey layer also is a strong argument against the hypothesis that oxygen depletion of
729 the bottom waters during glacial intervals would be the explanation for the low Mn
730 content in these intervals. The XRF-scanner data clearly show that most glacial
731 intervals still contain Mn, while the interval just below the grey layer is close to zero,
732 evidently because of dissolution of Mn under anoxic conditions.

733 The formation of the thin, horizontal Mn layers is more enigmatic. The
734 horizontal closely spaced banding and the presence of repeated layers of frost-like
735 crystals clearly show that these layers must have formed by repeated shifts in the
736 position of the redox boundary, and that the redox boundary was situated well below
737 any active bioturbation. However, why the redox boundary fluctuated strongly in

738 certain intervals is presently unclear. We can only speculate that intermittent inflow of
739 well-oxygenated waters during glacial intervals resulted in the repeated diffusion of
740 oxygen into dysoxic pore waters and controlled the formation of these layers.

741 **6 Conclusions**

742 The detailed observation of variations in type and intensity of bioturbation in
743 combination with high-resolution XRF-scanner data on Mn variations in sediment
744 cores from the Arctic Ocean allow a number of conclusions to be made:

- 745 • The Arctic deep-sea ichnofauna is sparse consisting primarily of *Planolites*,
746 *Trichichnus*, and *Chondrites*, locally abundant *Nereites*, and occasional
747 *Phycosiphon*, *Scolicia*, and *Zoophycos*. The trace fossil fauna suggest an
748 *Nereites* or *Zoohycos* ichnofacies.
- 749 • The spatial variability in trace fossil abundance and diversity agree with modern
750 patterns in the distribution of benthic organisms, indicating that the trace fossil
751 variability is strongly controlled by food flux, which is controlled by the
752 geographic positions in relation to continental shelf breaks and sea ice margin.
- 753 • Trace fossil abundance and diversity show strong glacial-interglacial variability.
- 754 • During interglacial periods the increased food flux rather than changes in deep
755 water circulation are responsible for the enhanced abundance and diversity in
756 the ichnofauna.
- 757 • In the glacial intervals, the impoverished ichnofauna consisting almost
758 exclusively of *Trichichnus* and *Chondrites* is a response to extremely low food
759 flux causing the burrowing organisms to use microbes to convert refractory
760 carbon in the sediment to a labile food source. The presence of trace fossil in the

761 glacial intervals also indicate that bottom water remained oxic even during peak
762 glacial.

- 763 • There is a close correlation between enhanced Mn content and increased trace
764 fossil size, abundance, and diversity. Exceptions are found in areas with strong
765 currents or extreme ice conditions even during interglacials.
- 766 • Detailed comparison of X-ray radiographs and XRF-scanner data show that Mn
767 deposited under interglacial conditions may be dissolved and precipitate on new
768 positions. Where the Mn has been dissolved, trace fossils can still be used to
769 positively identify the original position of the interglacial sediment.

770 Diagenetically precipitated layers of Mn show a distinct banding not present in
771 the interglacially deposited brown, Mn-rich layers. Thus, by using radiographs,
772 dissolved and diagenetically formed layers can be identified and accounted for
773 in stratigraphic correlations, allowing robust correlations over large distances in
774 the Arctic Ocean.

775 **7 Acknowledgments**

776 Matti Karlström, Anders Sundberg, and Helga Heilmann are cordially thanked
777 for their help in producing the radiographs. Mikael Hovemyr and Marianne Ahlbom
778 are thanked for performing microscope and SEM analysis. The Swedish Polar
779 Research Secretariat, the Swedish Research Council (VR), and the Knut and Alice
780 Wallenberg Foundation are thanked for supporting research cruises and laboratory
781 facilities.

782

783

784 **8 References**

- 785 Arrigo, K.R., Perovich, D.K., Pickart, R.S., Brown, Z.W., van Dijken, G.L., Lowry,
786 K.E., Mills, M.M., Palmer, M.A., Balch, W.M., Bahr, F., Bates, N.R., Benitez-
787 Nelson, C., Bowler, B., Brownlee, E., Ehn, J.K., Frey, K.E., Garley, R., Laney,
788 S.R., Lubelczyk, L., Mathis, J., Matsuoka, A., Mitchell, B.G., Moore, G.W.K.,
789 Ortega-Retuerta, E., Pal, S., Polashenski, C.M., Reynolds, R.A., Schieber, B.,
790 Sosik, H.M., Stephens, M., Swift, J.H., 2012. Massive Phytoplankton Blooms
791 Under Arctic Sea Ice. *Science*, DOI:10.1126/science.1215065.
- 792 Arrigo, K.R., van Dijken, G., Pabi, S., 2008. Impact of a shrinking Arctic ice cover on
793 marine primary production. *Geophysical Research Letters* 35(19), L19603.
- 794 Backman, J., Fornaciari, E., Rio, D., 2009. Biochronology and paleoceanography of
795 late Pleistocene and Holocene calcareous nannofossil abundances across the
796 Arctic Basin. *Marine Micropaleontology* 72(1-2), 86-98.
- 797 Backman, J., Jakobsson, M., Løvlie, R., Polyak, L., 2004. Is the central Arctic Ocean
798 a sediment starved basin? *Quaternary Science Reviews* 23, 1435-1454.
- 799 Barnes, D.K.A., Souster, T., 2011. Reduced survival of Antarctic benthos linked to
800 climate-induced iceberg scouring. *Nature Clim. Change* 1(7), 365-368.
- 801 Björk, G., Anderson, L., Jakobsson, M., Antony, D., Eriksson, P.B., Eriksson, B.,
802 Hell, B., Hjalmarsson, S., Janzen, T., Jutterström, S., Linders, J., Löwemark,
803 L., Marcussen, C., Olsson, K.A., Rudels, B., Sellén, E., Sølvesten, M., 2010.
804 Flow of Canadian Basin Deep Water in the Western Eurasian Basin of the
805 Arctic Ocean. *Deep Sea Research* 57(4), 577-58.
- 806 Björk, G., Jakobsson, M., Rudels, B., Swift, J.H., Anderson, L., Darby, D.A.,
807 Backman, J., Coakley, B., Winsor, P., Polyak, L., Edwards, M., 2007.
808 Bathymetry and deep-water exchange across the central Lomonosov Ridge at

809 88-89°N. Deep Sea Research Part I: Oceanographic Research Papers 54(8),
810 1197-1208.

811 Blanpied, C., Bellaiche, G., 1981. Bioturbation on the pelagic platform: Ichnofacies
812 variations as paleoclimatic indicator. Marine Geology 43, M49-M57.

813 Bluhm, B.A., MacDonald, I.R., Debenham, C., Iken, K., 2005. Macro- and
814 megabenthic communities in the high Arctic Canada Basin: initial findings.
815 Polar Biology 28(3), 218-231.

816 Bouma, A.H., 1964. Notes on X-ray interpretation of marine sediments. Marine
817 Geology 2, 278-309.

818 Bromley, R.G., 1991. *Zoophycos*: Strip mine, refuse dump, cache or sewage farm?
819 Lethaia 24, 460-462.

820 Bromley, R.G., 1996. Trace Fossils: Biology, Taphonomy and Applications.
821 Chapman and Hall, London, 361 pp.

822 Burdige, D., 2006. Geochemistry of marine sediments. Princeton University Press,
823 Princeton, NJ, USA, 609 pp.

824 Clark, D.L., 1970. Magnetic Reversals and Sedimentation Rates in the Arctic Ocean.
825 Geological Society of America Bulletin 81(10), 3129-3134.

826 Clark, D.L., Whitman, R.R., Morgan, K.A., Mackey, S.D., 1980. Stratigraphy and
827 Glacial-Marine Sediments of the Amerasian Basin, Central Arctic Ocean. The
828 Geological Society of America. Special Paper 181, 1-57.

829 Clough, L.M., Ambrose, J.W.G., Kirk Cochran, J., Barnes, C., Renaud, P.E., Aller,
830 R.C., 1997. Infaunal density, biomass and bioturbation in the sediments of the
831 Arctic Ocean. Deep Sea Research Part II: Topical Studies in Oceanography
832 44(8), 1683-1704.

833 Comiso, J.C., Nishio, F., 2008. Trends in the sea ice cover using enhanced and
834 compatible AMSR-E, SSM/I, and SMMR data. *J. Geophys. Res.* 113(C2),
835 C02S07.

836 Comiso, J.C., Parkinson, C.L., Gersten, R., Stock, L., 2008. Accelerated decline in the
837 Arctic sea ice cover. *Geophysical Research Letters* 35(1), L01703.

838 Cronin, T.M., Gemery, L., Briggs Jr, W.M., Jakobsson, M., Polyak, L., Brouwers,
839 E.M., 2010. Quaternary Sea-ice history in the Arctic Ocean based on a new
840 Ostracode sea-ice proxy. *Quaternary Science Reviews* 29(25-26), 3415-3429.

841 Croudace, I.W., Rindby, A., Rothwell, R.G., 2006. ITRAX: description and
842 evaluation of a new multi-function X-ray core scanner. In: R.G. Rothwell
843 (Editor), *New techniques in sediment core analysis*. Geological Society of
844 London, London, pp. 51-63.

845 Deubel, H., 2000. Structures and nutrition requirements of macrozoobenthic
846 communities in the area of the Lomonossov Ridge in the Arctic Ocean.
847 *Reports on Polar Research* 370, 1-147.

848 Ekdale, A.A., 1985. Paleoecology of the marine endobenthos. *Palaeogeography,*
849 *Palaeoclimatology, Palaeoecology* 50, 63-81.

850 Ekdale, A.A., Mason, T.R., 1988. Characteristic trace-fossil associations in oxygen-
851 poor sedimentary environments. *Geology* 16, 720-723.

852 Emery, K.O., Hülsemann, J., 1964. Shortening of sediment cores collected in open-
853 barrel gravity corers. *Sedimentology* 3, 144-154.

854 Eriksson, J., O'Regan, M., Löwemark, L., submitted. Authigenic minerals in
855 Quaternary sediments from the Amerasian Basin: Do they bias stratigraphic
856 and paleo-environmental interpretations?

857 Frey, R.W., Pemberton, S.G., 1984. Trace fossil facies models. In: R.G. Walker
858 (Editor), *Facies Models*. Geoscience Canada, pp. 189-207.

859 Froehlich, P.N., Klinkhammer, G.P., Bender, M.L., Luedtke, N.A., Heath, G.R.,
860 Cullen, D., Dauphin, P., Hammond, D., Hartman, B., 1979. Early oxygenation
861 of organic matter in pelagic sediments of the eastern equatorial Atlantic:
862 suboxic diagenesis. *Geochimica et Cosmochimica Acta* 43, 1075-1090.

863 Fu, S., 1991. Funktion, Verhalten und Einteilung fucoider und lophocteniider
864 Lebensspuren, Courier Forschungsinstitut Senckenberg. Senckenbergische
865 Naturforschende Gesellschaft Frankfurt a. M., pp. 1-79.

866 Fu, S., Werner, F., 1994. Distribution and composition of biogenic structures on the
867 Iceland-Faeroe Ridge: Relation to different environments. *Palaios* 9, 92-101.

868 Fu, S., Werner, F., 1995. Is *Zoophycos* a feeding trace? *Neues Jahrbuch für Geologie
869 und Paläontologie* 195(1-3), 37-47.

870 Fu, S., Werner, F., 2000. Distribution, ecology and taphonomy of the organism trace,
871 *Scolicia*, in northeast Atlantic deep-sea sediments. *Palaeogeography,
872 Palaeoclimatology, Palaeoecology* 156, 289–300.

873 Gong, Y.-M., Shi, G.R., Weldon, E.A., Du, Y.-S., Xu, R., 2008. Pyrite framboids
874 interpreted as microbial colonies within the Permian *Zoophycos* spreiten from
875 southeastern Australia. *Geological Magazine* 145(1), 95–103.

876 Haley, B.A., Frank, M., Spielhagen, R.F., Eisenhauer, A., 2008. Influence of brine
877 formation on Arctic Ocean circulation over the past 15 million years. *Nature
878 Geosci* 1(1), 68-72.

879 Horner, R.A., Schrader, G.C., 1982. Relative contributions of ice algae,
880 phytoplankton, and benthic microalgae to primary production in nearshore
881 regions of the Beaufort Sea. *Arctic* 35, 484-503.

882 Iken, K., Bluhm, B.A., Gradinger, R., 2005. Food web structure in the high Arctic
883 Canada Basin: evidence from $\delta^{13}\text{C}$ and $\delta^{15}\text{N}$ analysis. *Polar Biology* 28(3),
884 238-249.

885 Jakobsson, M., Grantz, A., Kristoffersen, Y., Macnab, R., 2003. Physiographic
886 provinces of the Arctic Ocean seafloor. *GSA Bulletin* 115(12), 1443-1455.

887 Jakobsson, M., Løvlie, R., Al-Hanbali, H., Arnold, E., Backman, J., Mörth, M., 2000.
888 Manganese and color cycles in Arctic Ocean sediments constrain Pleistocene
889 chronology. *Geology* 28, 23-26.

890 Jakobsson, M., Macnab, R., Mayer, L., Anderson, R., Edwards, M., Hatzky, J.,
891 Schenke, H.W., Johnson, P., 2008. An improved bathymetric portrayal of the
892 Arctic Ocean: Implications for ocean modeling and geological, geophysical
893 and oceanographic analyses. *Geophysical Research Letters* 35, L07602,
894 doi:10.1029/2008GL033520.

895 Jakobsson, M., Nilsson, J., O'Regan, M., Backman, J., Löwemark, L., Dowdeswell,
896 J.A., Mayer, L., Polyak, L., Colleoni, F., Anderson, L.G., Björk, G., Darby,
897 D., Eriksson, B., Hanslik, D., Hell, B., Marcussen, C., Sellén, E., Wallin, Å.,
898 2010. An Arctic Ocean ice shelf during MIS 6 constrained by new geophysical
899 and geological data. *Quaternary Science Reviews* 29, 3505-3517.

900 Johnson, K.S., Coale, H.K., Berelson, W.M., Gordon, R.M., 1996. On the formation
901 of the manganese maximum in the oxygen minimum. *Geochimica et*
902 *Cosmochimica Acta* 60(8), 1291-1299.

903 Jokat, W., Uenzelmann-Neben, G., Kristoffersen, Y., Rasmussen, T.M., 1992.
904 Lomonosov Ridge--A double-sided continental margin. *Geology* 20(10), 887-
905 890.

- 906 Kitchell, J.A., 1979. Deep-sea foraging pathways: an analysis of randomness and
907 resource exploitation. *Paleobiology* 5, 107-125.
- 908 Kitchell, J.A., Kitchell, J.F., Johnson, G.L., Hunkins, K.L., 1978. Abyssal traces and
909 megafauna: comparison of productivity, diversity and density in the Arctic and
910 Antarctic. *Paleobiology* 4(2), 171-180.
- 911 Kotake, N., 1997. Ethological interpretation of the trace fossil *Zoophycos* in the
912 Hikoroichi Formation (Lower Carboniferous), southern Kitakama Mountains,
913 Northeast Japan. *Paleontological Research* 1(1), 15-28.
- 914 Kröncke, I., 1994. Macrobenthos composition, abundance and biomass in the Arctic
915 Ocean along a transect between Svalbard and the Makarov Basin. *Polar*
916 *Biology* 14, 519-529.
- 917 Kröncke, I., 1998. Macrofauna communities in the Amundsen Basin, at the Morris
918 Jesup Rise and at the Yermak Plateau (Eurasian Arctic Ocean). *Polar Biology*
919 19(6), 383-392.
- 920 Lapina, N.N., 1965. The determination of distribution paths of sediments, based on
921 mineralogical investigations of marine deposits(example Laptev Sea).
922 *Uchennye Zapiski NIIGA. Serie Regional Geology* 7, 139-157.
- 923 Levin, L.A., Etter, R.J., Rex, M.A., Gooday, A.J., Smith, C.R., Pineda, J., Stuart,
924 C.T., Hessler, R.R., Pawson, D., 2001. Environmental influences on regional
925 deep-sea species diversity. *Annual Review of Ecological Systems* 32(1), 51-93.
- 926 Levitan, G., Burtman, M.B., Tarasov, N., Kukina, N.A., 1999. Mineral Composition
927 of the St. Anna Trough Surface Sediments. *Oceanology* 39(6), 821-829.
- 928 Li, Y.-H., Bischoff, J., Mathieu, G., 1969. The migration of manganese in the arctic
929 basin sediment. *Earth and Planetary Science Letters* 7(3), 265-270.

930 Löwemark, L., 2003. Automatic image analysis of X-ray radiographs: a new method
931 for ichnofabric evaluation. *Deep-Sea Research I* 50, 815-827.

932 Löwemark, L., 2012. Ethological analysis of the trace fossil *Zoophycos*: Hints from
933 the Arctic Ocean. *Lethaia*(45), 290–298. DOI: 10.1111/j.1502-
934 3931.2011.00282.x.

935 Löwemark, L., Jakobsson, M., Mörth, M., Backman, J., 2008. Arctic Ocean Mn
936 contents and Sediment Color Cycles. *Polar Research* 27, 105–113.

937 Löwemark, L., Schäfer, P., 2003. Ethological implications from a detailed X-ray
938 radiograph and ¹⁴C-study of the modern deep-sea *Zoophycos*.
939 *Palaeogeography, Palaeoclimatology, Palaeoecology* 192(1-4), 101-121.

940 Löwemark, L., Schönfeld, J., Schäfer, P., 2006. Deformation of pyritized burrows: A
941 novel technique for the detection and quantification of core shortening in
942 gravity cores. *Marine Geology* 233, 37–48.

943 Löwemark, L., Schönfeld, J., Werner, F., Schäfer, P., 2004. Trace fossils as a
944 paleoceanographic tool: evidence from Late Quaternary sediments of the
945 southwestern Iberian margin. *Marine Geology* 204(1-2), 27-41.

946 Löwemark, L., Werner, F., 2001. Dating errors in high-resolution stratigraphy: a
947 detailed X-ray radiograph and AMS-¹⁴C study of *Zoophycos* burrows. *Marine*
948 *Geology* 177(3-4), 191-198.

949 MacDonald, I.R., Bluhm, B.A., Iken, K., Gagaev, S., Strong, S., 2010. Benthic
950 macrofauna and megafauna assemblages in the Arctic deep-sea Canada Basin.
951 *Deep Sea Research Part II: Topical Studies in Oceanography* 57(1-2), 136-
952 152.

953 Macdonald, R., Gobeil, C., 2011. Manganese Sources and Sinks in the Arctic Ocean
954 with Reference to Periodic Enrichments in Basin Sediments. *Aquatic*
955 *Geochemistry*, 1-27.

956 Martin, J.H., Knauer, G.A., 1980. Manganese cycling in northeast Pacific waters.
957 *Earth and Planetary Science Letters* 51(2), 266-274.

958 Mashiotta, T.A., Lea, D.W., Spero, H.J., 1999. Glacial-interglacial changes in
959 Subantarctic sea surface temperature and ^{18}O -water using foraminiferal Mg.
960 *Earth and Planetary Science Letters* 170, 417-432.

961 McBride, E.F., Picard, M.D., 1991. Facies implications of *Trichichnus* and *Chondrites*
962 in turbidites and hemipelagites, Marnoso-arenacea formation (Miocene),
963 Northern Apennines, Italy. *Palaios* 6(3), 281-290.

964 Meincke, J., Rudels, B., Friedrich, H.J., 1997. The Arctic Ocean–Nordic Seas
965 thermohaline system. *ICES Journal of Marine Science: Journal du Conseil*
966 54(3), 283-299.

967 Middag, R., de Baar, H.J.W., Laan, P., Klunder, M.B., 2011. Fluvial and
968 hydrothermal input of manganese into the Arctic Ocean. *Geochimica et*
969 *Cosmochimica Acta* 75(9), 2393-2408.

970 März, C., Stratmann, A., Matthiessen, J., Meinhardt, A.K., Eckert, S., Schnetger, B.,
971 Vogt, C., Stein, R., Brumsack, H.J., 2011. Manganese-rich brown layers in
972 Arctic Ocean sediments: Composition, formation mechanisms, and diagenetic
973 overprint. *Geochimica et Cosmochimica Acta* 75, 7668–7687. doi:
974 10.1016/j.gca.2011.09.046.

975 O'Regan, M., 2011. Late Cenozoic Paleoceanography of the Central Arctic Ocean.
976 IOP conference Series- Earth and Environmental Sciences (IODP Summer
977 school special volume) 14, doi:10.1088/1755-1315/14/1/012002.

978 O'Regan, M., King, J., Backman, J., Jakobsson, M., Pälike, H., Moran, K., Heil, C.,
979 Sakamoto, T., Cronin, T.M., Jordan, R.W., 2008. Constraints on the
980 Pleistocene chronology of sediments from the Lomonosov Ridge.
981 *Paleoceanography* 23, PA1S19, doi:10.1029/2007PA001551.

982 O'Regan, M., St. John, K., Moran, K., Backman, K., King, J., Haley, B.A., Jakobsson,
983 M., F., M., R., U., 2010. Plio-Pleistocene trends in ice rafted debris on the
984 Lomonosov Ridge. *Quaternary International* 219, 168-176.
985 doi:10.1016/j.quaint.2009.08.010.

986 Olivero, D., 1995. La trace fossile *Zoophycos* Massalongo 1855. Historique et
987 interprétations actuelles. *Bollettino Museo Regionale di Scienze Naturali*
988 *Torino* 13(1), 5-34.

989 Phillips, L.R., Grantz, A., 1997. Quaternary history of sea ice and paleoclimate in the
990 Amerasia basin, Arctic Ocean, as recorded in the cyclical strata of Northwind
991 Ridge. *Geological Society of America Bulletin* 109(9), 1101-1115.

992 Phillips, R.L., Grantz, A., 2001. Regional variations in provenance and abundance of
993 ice-rafted clasts in Arctic Ocean sediments: implications for the configuration
994 of late Quaternary oceanic and atmospheric circulation in the Arctic. *Marine*
995 *Geology* 172(1-2), 91-115.

996 Piepenburg, D., 2005. Recent research on Arctic benthos: common notions need to be
997 revised. *Polar Biology* 28(10), 733-755.

998 Poirier, R.K., Cronin, T.M., Briggs Jr, W.M., Lockwood, R., 2012. Central Arctic
999 paleoceanography for the last 50 kyr based on ostracode faunal assemblages.
1000 *Marine Micropaleontology* 88–89(0), 65-76.

1001 Polyak, L.V., 1986. New data on microfauna and stratigraphy of bottom sediments

1002 of the Mendeleev Ridge, Arctic ocean. In: S.I. Andreyev (Editor), The genesis of
1003 sediments and formation of nodules in the ocean. Sevmorgeologia, Leningrad,
1004 pp. 40-50.

1005 Poore, R.Z., Phillips, R.L., Rieck, H.J., 1993. Paleoclimate Record for Northwind
1006 Ridge, Western Arctic Ocean. *Paleoceanography* 8(2), 149-159.

1007 Rachold, V., (, e., Springer, B., 199-222., 1999. Major, trace, and rare earth element
1008 geochemistry of suspended particulate material of East Siberian rivers draining
1009 to the Arctic Ocean, Land-ocean systems in the Siberian Arctic:. In: H.
1010 Kassens, H.A. Bauch, I. Dmitrenko, H. Eicken, H.-W. Hubberten, M. Melles,
1011 J. Thiede, L.A. Timokhov (Editors), Dynamics and history.

1012 Renaud, P.E., Ambrose, J.W.G., Vanreusel, A., Clough, L.M., 2006. Nematode and
1013 macrofaunal diversity in central Arctic Ocean benthos. *Journal of*
1014 *Experimental Marine Biology and Ecology* 330(1), 297-306.

1015 Romero-Wetzel, M.B., 1987. Sipunculans as inhabitants of very deep, narrow
1016 burrows in deep-sea sediments. *Marine Biology (Historical Archive)* 96(1),
1017 87-91.

1018 Rudels, B., Jones, E.P., Schauer, U., Eriksson, P., 2004. Atlantic sources of the Arctic
1019 Ocean surface and halocline waters. *Polar Research* 23(2), 181-208.

1020 Savrda, C.E., 2007. Trace fossils and marine benthic oxygenation. In: W. Miller III
1021 (Editor), Trace fossils: Concepts, problems, prospects. Elsevier, Amsterdam,
1022 pp. 149-158.

1023 Savrda, C.E., Bottjer, D.J., 1986. Trace-fossil model for reconstruction of paleo-
1024 oxygenation in bottom waters. *Geology* 14, 3-6.

1025 Savrda, C.E., Bottjer, D.J., 1989. Trace-fossil model for reconstructing oxygenation
1026 histories of ancient marine bottom waters: Application to Upper Cretaceous

- 1027 Niobrara formation, Colorado. *Palaeogeography, Palaeoclimatology,*
1028 *Palaeoecology* 74, 49-74.
- 1029 Schnack, K., 1998. Besiedlungsmuster der benthischen Makrofauna auf dem
1030 ostgrönländischen Kontinentalhang. *Berichte zur Polarforschung* 294, 1-124.
- 1031 Scott, D.B., Mudie, P.J., Baki, V., Mackinnon, K.D., Cole, F.E., 1989.
1032 Biostratigraphy and late Cenozoic paleoceanography of the Arctic Ocean:
1033 Foraminiferal, lithostratigraphic, and isotopic evidence. *Geological Society of*
1034 *America Bulletin* 101, 260-277. doi: 10.1130/0016-7606.
- 1035 Seilacher, A., 1962. Paleontological studies on turbidite sedimentation and erosion.
1036 *Journal of Geology* 70(2), 227-233.
- 1037 Seilacher, A., 1964. Biogenic sedimentary structures. In: J. Imbrie, N. Newell
1038 (Editors), *Approaches to Paleoecology*. John Wiley and Sons, New York, pp.
1039 296-316.
- 1040 Seilacher, A., 1967. Bathymetry of trace fossils. *Marine Geology* 5, 413-428.
- 1041 Seilacher, A., 1990. Aberrations in bivalve evolution related to photo- and chemo
1042 symbiosis. *Historical Biology* 3, 289-311.
- 1043 Sellén, E., Jakobsson, M., Backman, J., 2008. Sedimentary regimes in Arctic's
1044 Amerasian and Eurasian Basins: Clues to differences in sedimentation rates.
1045 *Global and Planetary Change* 61, 275–284.
- 1046 Sellén, E., Jakobsson, M., Frank, M., Kubik, P.W., 2009. Pleistocene variations of
1047 beryllium isotopes in central Arctic Ocean sediment cores. *Global and*
1048 *Planetary Change* 68(1-2), 38-47.
- 1049 Sellén, E., O'Regan, M., Jakobsson, M., 2010. Spatial and temporal Arctic Ocean
1050 depositional regimes: a key to the evolution of ice drift and current patterns.
1051 *Quaternary Science Reviews* 29(25-26), 3644-3664.

1052 Spielhagen, R.F., Baumann, K.-H., Erlenkeuser, H., Nowaczyk, N.R., Nørgaard-
1053 Pedersen, N., Vogt, C., Weiel, D., 2004. Arctic Ocean deep-sea record of
1054 northern Eurasian ice sheet history. *Quaternary Science Reviews* 23 1455-
1055 1483.

1056 Stein, R., 2008. Arctic ocean sediments: processes, proxies, and paleoenvironment.
1057 *Developments in Marine Geology*. Elsevier, Amsterdam, 608 pp.

1058 Svindland, K.T., Vorren, T.O., 2002. Late Cenozoic sedimentary environments in the
1059 Amundsen Basin, Arctic ocean. *Marine Geology* 186, 541-555.

1060 Taldenkova, E., Bauch, H.A., Gottschalk, J., Nikolaev, S., Rostovtseva, Y., Pogodina,
1061 I., Ovsepyan, Y., Kandiano, E., 2010. History of ice-rafting and water mass
1062 evolution at the northern Siberian continental margin (Laptev Sea) during Late
1063 Glacial and Holocene times. *Quaternary Science Reviews* 29, 3919e393.

1064 Tomczak, M., Godfrey, J.S., 2002. Arctic oceanography; the path of North Atlantic
1065 Deep Water, *Regional Oceanography: an introduction*. Pergamon, pp. 83-104.

1066 Tyszka, J., 1994. Paleoenvironmental implications from ichnological and microfaunal
1067 analyses of Bajocian spotty carbonates, Pieniny Klippen Belt, Polish
1068 Carpathians. *Palaios* 9(2), 175-187.

1069 Wahsner, M., Müller, C., Stein, R., Ivanov, G., Michael Levitan, Shelekhova, E.,
1070 Tarasov, G., 1999. Clay-mineral distribution in surface sediments of the
1071 Eurasian Arctic Ocean and continental margin as indicator for source areas
1072 and transport pathways - a synthesis. *Boreas* 28, 215-233.

1073 Van Averbeke, J., Martinez Arbizu, P., Dahms, H.U., Schminke, H.K., 1997. The
1074 metazoan meiobenthos along a depth gradient in the Arctic Laptev sea with
1075 special attentions to nematode communities. *Polar Biology* 18, 391-401.

1076 Vanreusel, A., Clough, L., Jacobsen, K., Ambrose, W., Jutamas, J., Ryheul, V.,
1077 Herman, R., Vincx, M., 2000. Meiobenthos of the central Arctic Ocean with
1078 special emphasis on the nematode community structure. Deep Sea Research
1079 Part I: Oceanographic Research Papers 47(10), 1855-1879.

1080 Werner, F., 1967. Röntgen-Radiographie zur Untersuchung von Sedimentstrukturen.
1081 Umschau in Wissenschaft und Technik 16, 532.

1082 Wetzel, A., 1991. Ecologic interpretation of deep-sea trace fossil communities.
1083 Palaeogeography, Palaeoclimatology, Palaeoecology 85, 47-69.

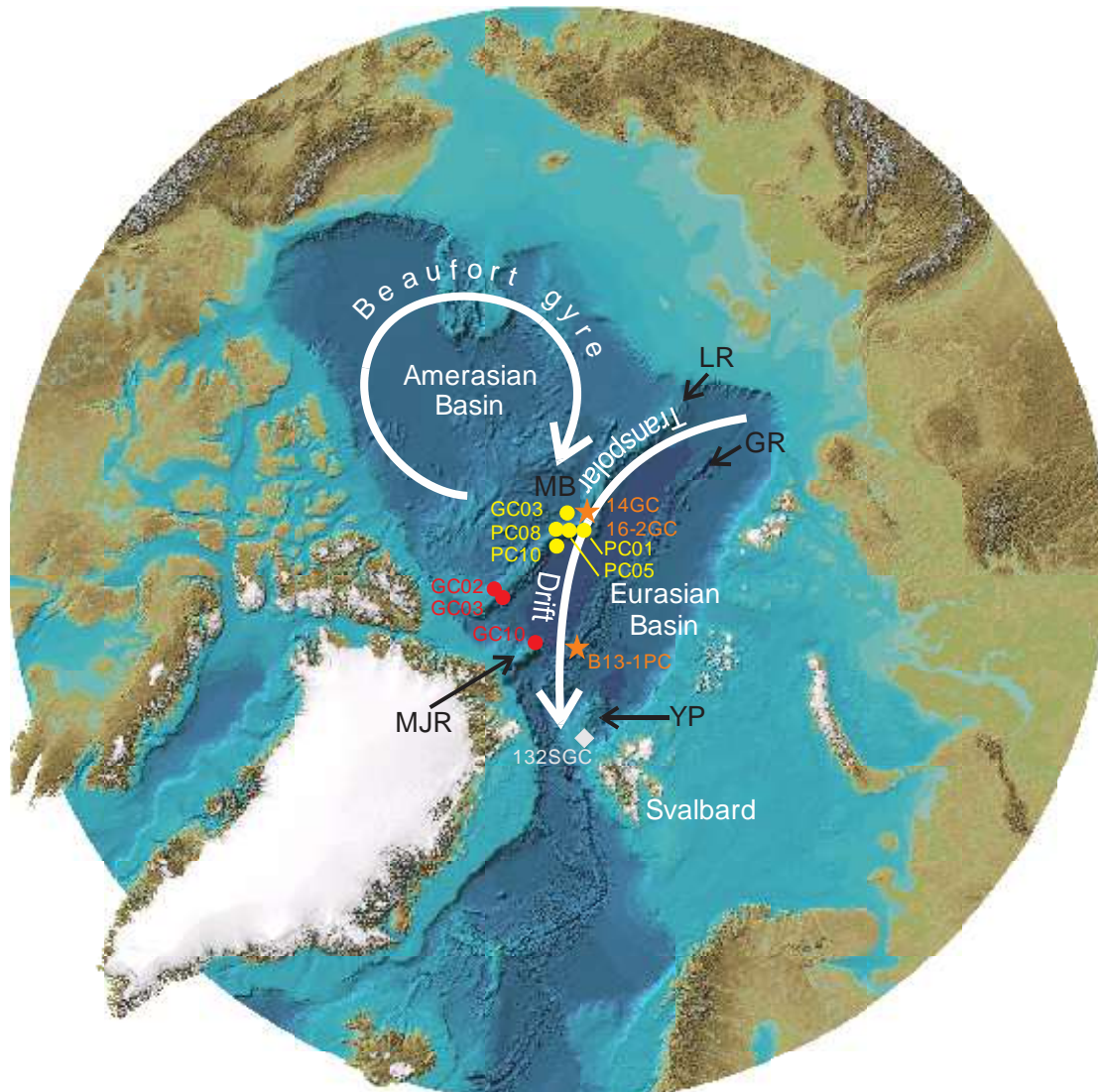
1084 Wetzel, A., 2002. Modern *Nereites* in the South China Sea-ecological association with
1085 redox conditions in the sediment. Palaios 17(5), 507-515.

1086 Wetzel, A., Wijayananda, N.P., 1990. Biogenic Sedimentary structures in outer
1087 Bengal Fan deposits drilled during Leg 116. Proceedings of the Ocean Drilling
1088 Program, Scientific Results 116, 15-24.

1089 Vogt, C., 1997. Regional and temporal variations of mineral assemblages in Arctic
1090 Ocean sediments as climatic indicator during glacial/interglacial changes.
1091 Reports on Polar Research 251, 1-309.

1092 Wollenburg, J.E., Kuhnt, W., 2000. The response of benthic foraminifers to carbon
1093 flux and primary production in the Arctic Ocean. Marine Micropaleontology
1094 40(3), 189-231.

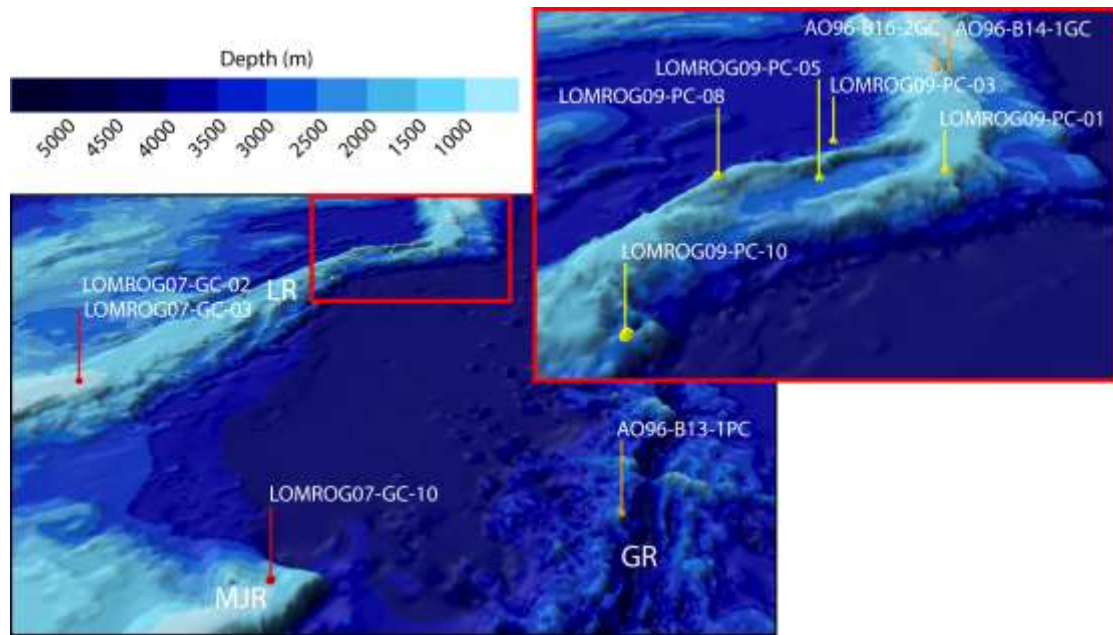
1095
1096
1097



1099

1100 **Fig. 1**

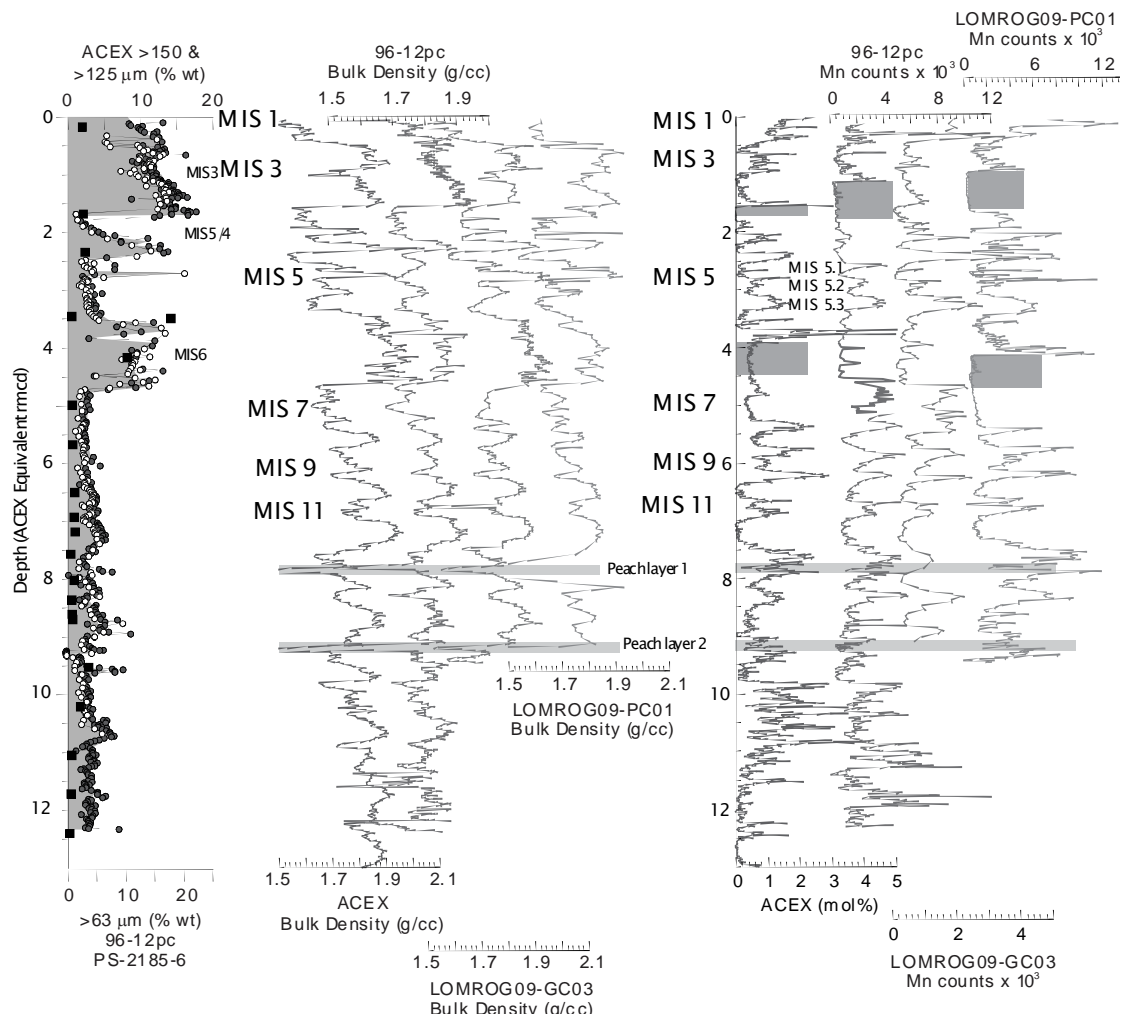
1101 Bathymetric chart of the Arctic Ocean (Jakobsson et al., 2008) showing the
 1102 positions of the studied cores and sea-ice circulation. GR=Gakkel Ridge,
 1103 LR=Lomonosov Ridge, MB=Makarov Basin, MJR=Morris Jesup Rise, YP=Yermak
 1104 Plateau. Grey diamond=YMER80 core, Orange stars=AO96-cores, Red
 1105 circles=LOMROG I-cores, Yellow circles=LOMROG II-cores



1106

1107 **Fig. 2**

1108 Digital elevation model showing the position of the cores relative to major
 1109 topographic features. Cores on the central Lomonosov Ridge show intense
 1110 bioturbation in interglacial intervals, while the cores on Morris Jesup Rise and the
 1111 Lomonosov Ridge off Greenland show sparse ichnofauna even during interglacial
 1112 periods.

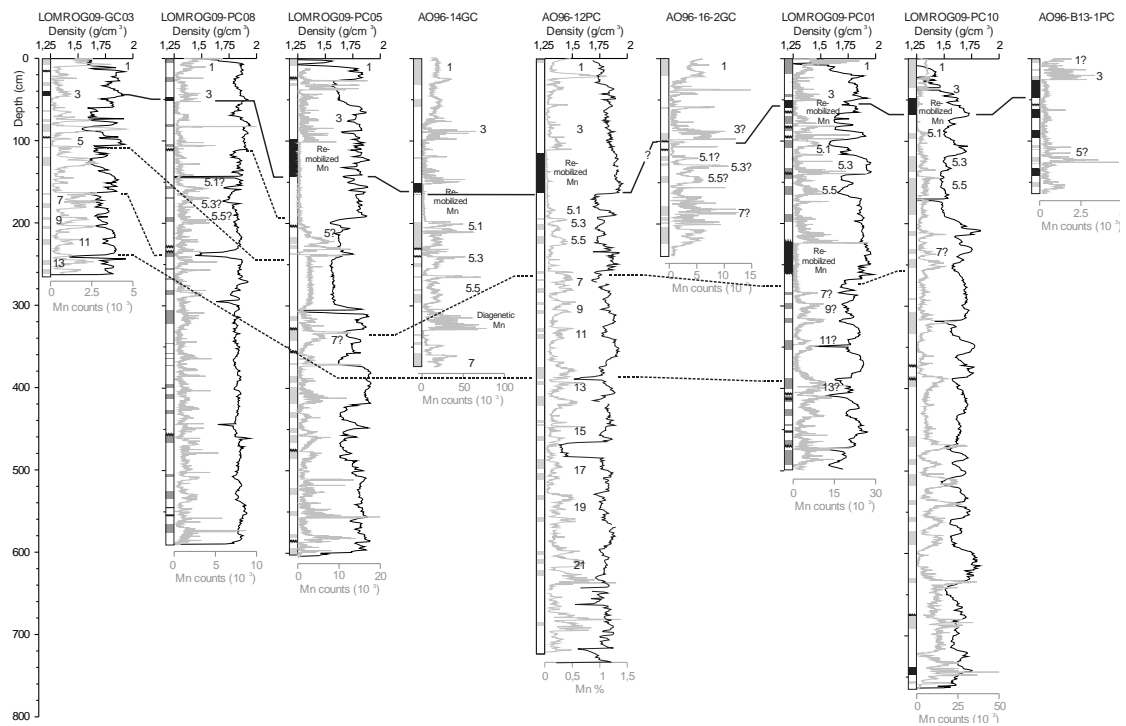


1113

1114 **Fig. 3**

1115 Correlations between central Lomonosov Ridge cores migrated onto the
 1116 ACEX depth scale to highlight the fidelity of the correlation using both bulk density
 1117 and relative Mn abundances. A) Stacked coarse fraction content records from ACEX
 1118 (>125 μm, black squares), AO-96-12pc (>63 μm, grey circles) and PS-2185-6 (>63
 1119 μm, open circles) showing the thick recurrent coarse grained diamictons found during
 1120 the last 2 glacial cycles B) Correlation of cores based on bulk density records
 1121 (O'Regan, 2011). Positions of MIS boundaries based on O'Regan et al. (2008),
 1122 Jakobsson et al. (2000) and Spielhagen et al. (2004). C) Correlation of Mn
 1123 abundances. Grey boxes indicate thickness and position of characteristic grey layers,

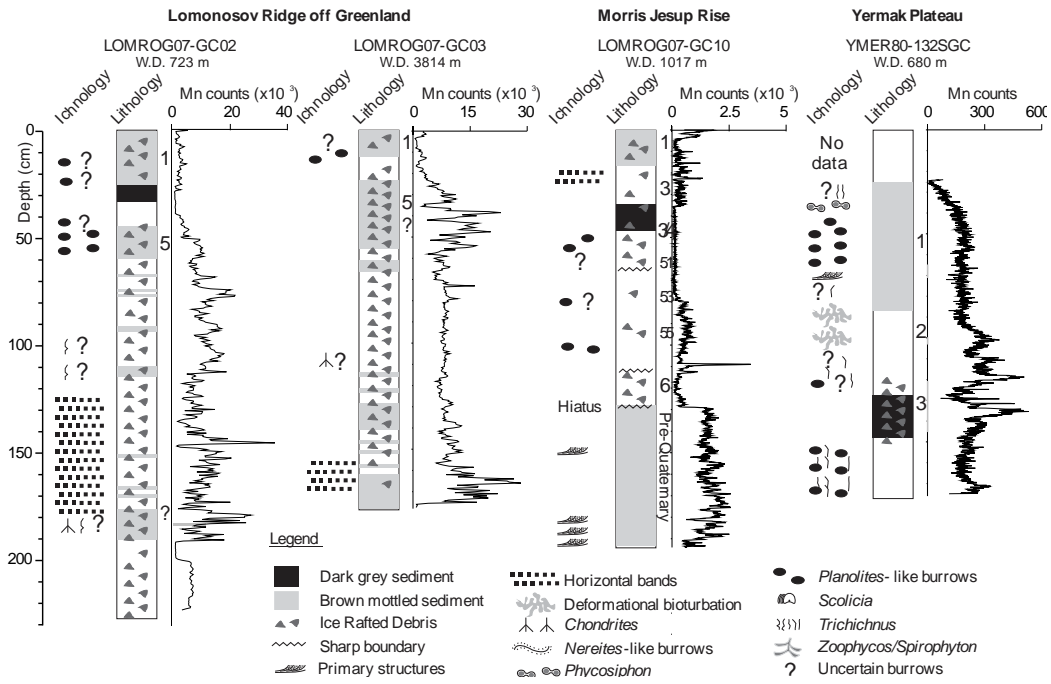
1124 which all show a depletion in Mn and possible redistribution of Mn in sediments
 1125 overlying the grey layer(s).



1126

1127 **Fig.4**

1128 Chronostratigraphic frame work for the studied cores. Correlations are made to
 1129 core AO96-12pc through lithological marker horizons, variations in Mn content and
 1130 distinct shifts in bulk density that can be followed over large areas. Correlations
 1131 between LOMROG09-GC03, and LOMROG09-PC01, AO96-12pc, and other cores
 1132 from the LR were published by O'Regan (2011). LOMROG09-PC08, and
 1133 LOMROG09-PC10 display a more complex pattern in downhole physical property
 1134 changes and prevents a detailed correlation below the grey layer marking the
 1135 boundary around MIS3/4. AO96-14gc, AO96-16-2gc, and LOMROG09-PC08 are
 1136 correlated based on characteristic Mn patterns surrounding the MIS 3/4 grey layer.



1137

1138 **Fig. 5**

1139 Variations in trace fossil content, simplified lithology, and Mn variations in

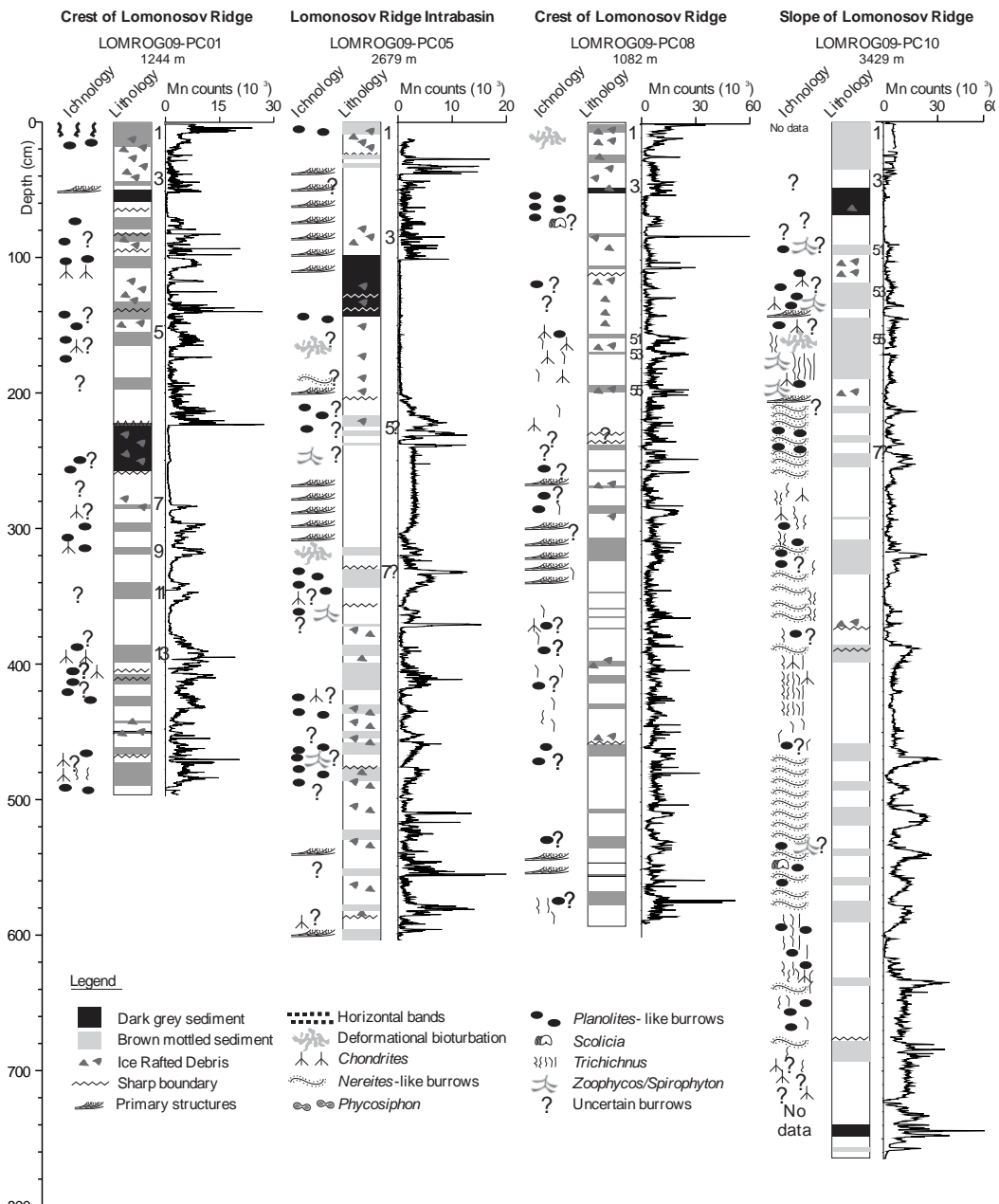
1140 the cores from the Lomonosov Ridge off Greenland, the Morris Jesup Rise, and the

1141 Yermak Plateau. Numbers between lithology and Mn log indicate marine isotope

1142 stages. The cores from the Lomonosov Ridge and Morris Jesup Rise contain

1143 diagenetic Mn layers, high levels of IRD, and sparse bioturbation focused to MIS 1

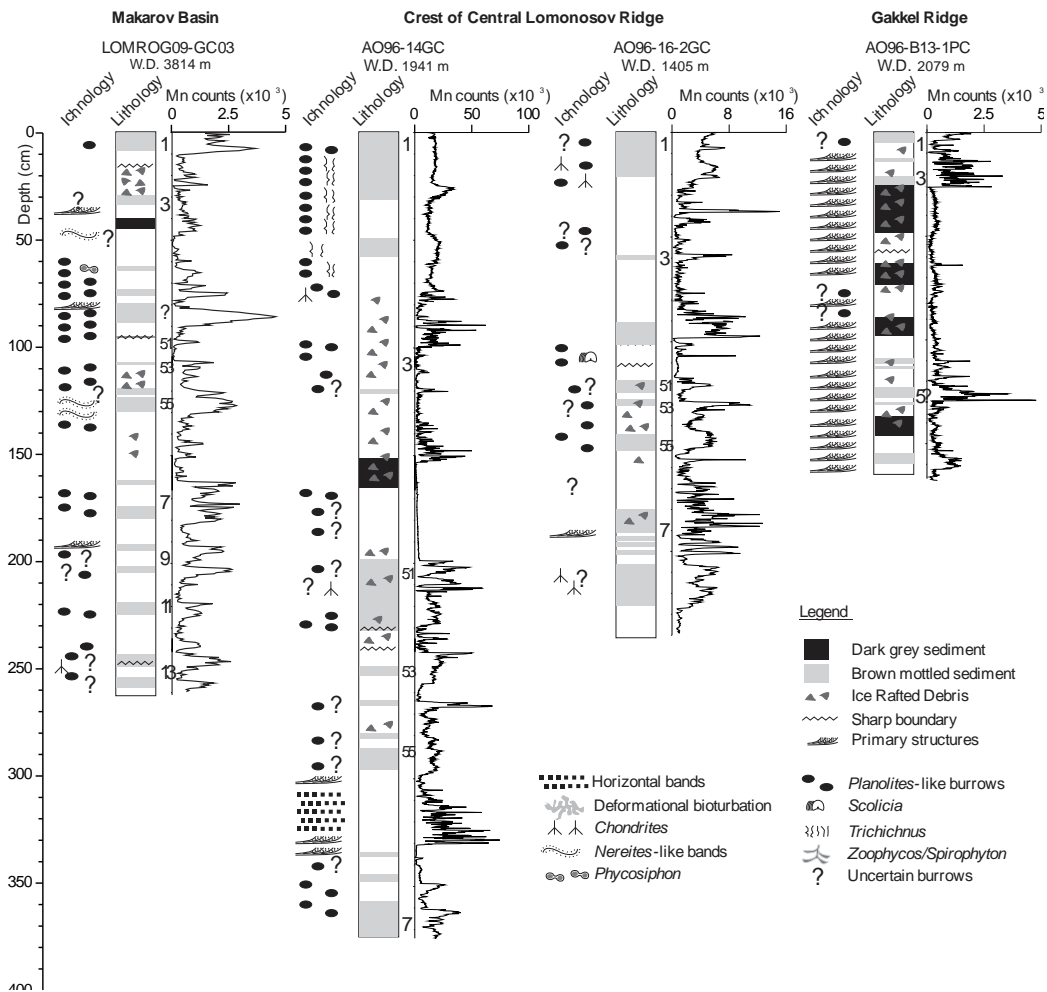
1144 and 5.



1145

1146 **Fig. 6**

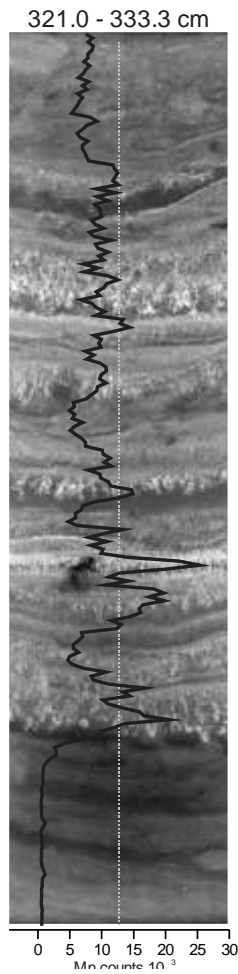
1147 Variations in trace fossil content, simplified lithology, and Mn variations in
 1148 the cores from the central Arctic Ocean on the Lomonosov Ridge. Numbers between
 1149 lithology and Mn log indicate marine isotope stages.



1150

1151 **Fig. 7**

1152 Variations in trace fossil content, simplified lithology, and Mn variations in
 1153 the cores from the Makarov Basin, central Lomonosov Ridge, and the Gakkel Ridge.
 1154 Numbers between lithology and Mn log indicate marine isotope stages.



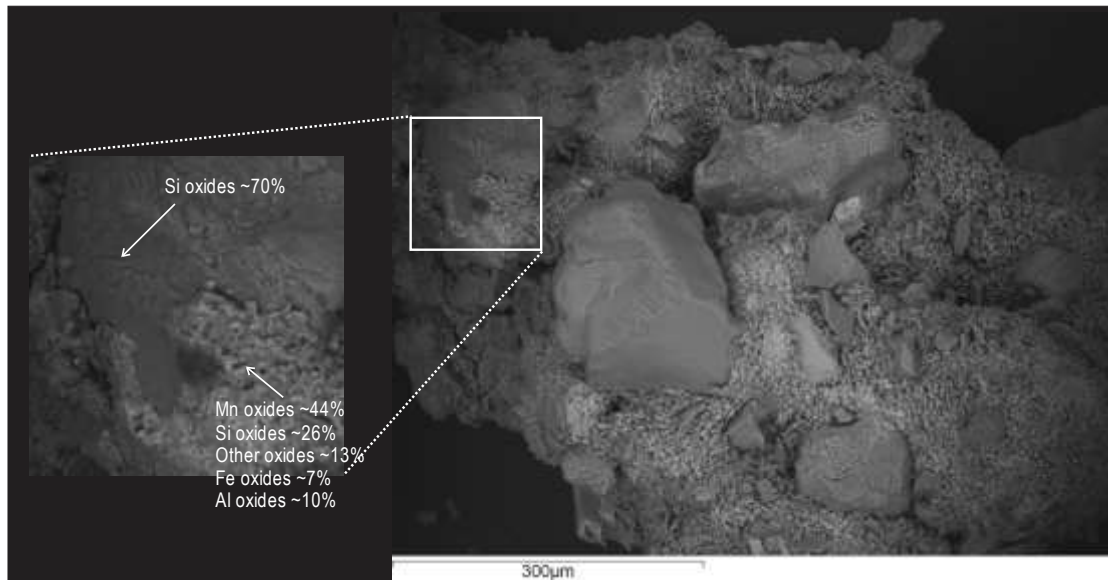
1155

1156 **Fig. 8**

1157 Layers of denser material appear as lighter as light bands in the X-ray

1158 radiographs. XRF-scans demonstrate that these layers contain strongly enhanced

1159 levels of Mn.

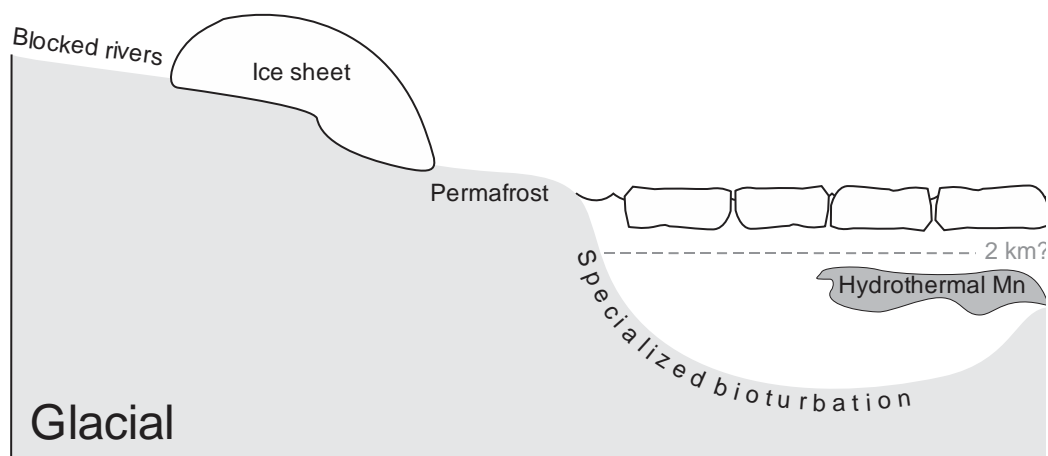
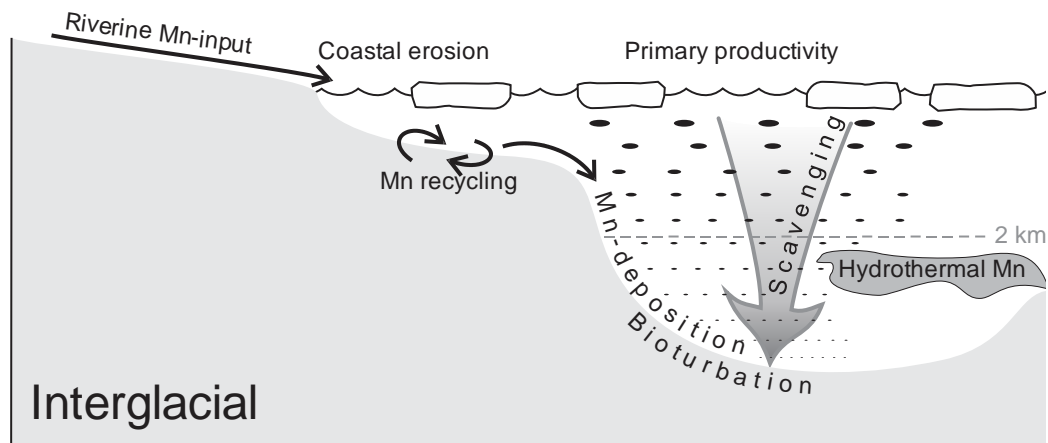


1160

1161 **Fig. 9**

1162 SEM-analysis of grains taken from the crystal-like layers shows that they are
1163 aggregates of Si-grains held together by a matrix of Mn minerals.

1164

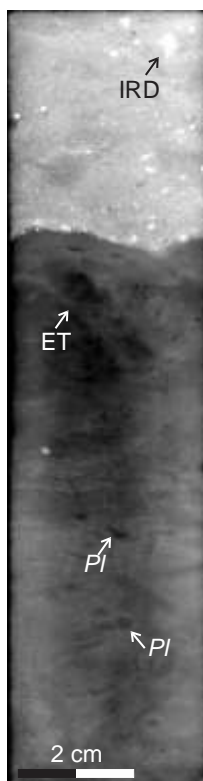


1165

1166 **Fig. 10**

1167 Conceptual model for the formation of Mn-rich layers during interglacials, and Mn-
 1168 poor layers during glacial periods. During interglacial conditions, the Mn budget is
 1169 controlled by the input of Mn from Arctic rivers and coastal erosion on the shelves
 1170 (Macdonald and Gobeil, 2011). On the shelves, the Mn goes through a number of
 1171 redox cycles before entering the ocean basin where scavenging by organic particles
 1172 helps to effectively bring the Mn to the sea floor (Johnson et al., 1996; Martin and
 1173 Knauer, 1980). The increased primary productivity also supports abundant and
 1174 diverse benthic activities. Hydrothermal Mn is of local importance, but is today not
 1175 detected above 2km water depth, lending little support to the idea that the Mn on the
 1176 upper slopes should be of hydrothermal origin.

1177 During glacial periods, the Arctic rivers are blocked by continental ice sheets, and Mn
1178 on the exposed shelves is stored in the permafrost, drastically reducing Mn input. The
1179 severe pack ice decreases primary productivity, and thus reduces both scavenging of
1180 Mn from the water column and the benthic activity on the sea floor. The trace fossils
1181 left in glacial sediments therefore represent specialized behaviours to utilized
1182 refractory carbon deep in the substrate. Hydrothermal Mn input likely was of minor
1183 influence.



1184

1185 **Fig. 11**

1186 X-ray radiograph from AO96-14GC (162.3-176cm) showing the base of the grey
1187 layer and the underlying intensely bioturbated sediment. A few cm under the sharp
1188 boundary an escape trace can be seen. ET = escape trace, *Pl* = *Planolites*, IRD = ice
1189 rafted debris